High order numerical schemes for linear elasticity

Tavelli Maurizio and Michael Dumbser

University of Trento

21-25 May 2018

Governing equations

$$
\begin{aligned}
\frac{\partial}{\partial t}\sigma_{xx} - \frac{\partial}{\partial x}u - \lambda\frac{\partial}{\partial y}v - \lambda\frac{\partial}{\partial z}w &= 0,\\
\frac{\partial}{\partial t}\sigma_{yy} - \lambda\frac{\partial}{\partial x}u - (\lambda+2\mu)\frac{\partial}{\partial y}v - \lambda\frac{\partial}{\partial z}w &= 0,\\
\frac{\partial}{\partial t}\sigma_{zz} - \lambda\frac{\partial}{\partial x}u - \lambda\frac{\partial}{\partial y}v - (\lambda+2\mu)\frac{\partial}{\partial z}w &= 0,\\
\frac{\partial}{\partial t}\sigma_{xy} - \mu\left(\frac{\partial}{\partial x}v + \frac{\partial}{\partial y}u\right) &= 0,\\
\frac{\partial}{\partial t}\sigma_{yz} - \mu\left(\frac{\partial}{\partial z}v + \frac{\partial}{\partial y}w\right) &= 0,\\
\frac{\partial}{\partial t}\sigma_{xz} - \mu\left(\frac{\partial}{\partial z}u + \frac{\partial}{\partial x}w\right) &= 0,\\
\frac{\partial}{\partial t}(\rho u) - \frac{\partial}{\partial x}\sigma_{xx} - \frac{\partial}{\partial y}\sigma_{xy} - \frac{\partial}{\partial z}\sigma_{xz} &= 0,\\
\frac{\partial}{\partial t}(\rho v) - \frac{\partial}{\partial x}\sigma_{xy} - \frac{\partial}{\partial y}\sigma_{yy} - \frac{\partial}{\partial z}\sigma_{yz} &= 0,\\
\frac{\partial}{\partial t}(\rho w) - \frac{\partial}{\partial x}\sigma_{xz} - \frac{\partial}{\partial y}\sigma_{yz} - \frac{\partial}{\partial z}\sigma_{zz} &= 0.
\end{aligned}
$$

$$
\boldsymbol{\sigma} = \begin{pmatrix} \sigma_{xx} & \sigma_{xy} & \sigma_{xz} \\ \sigma_{xy} & \sigma_{yy} & \sigma_{yz} \\ \sigma_{xz} & \sigma_{yz} & \sigma_{zz} \end{pmatrix} = \boldsymbol{\sigma}^T.
$$

$\mathbf{v} = (u, v, w)$ is the velocity field

ρ is the density

λ, μ are the classical Lamé constants

Governing equations

$$\frac{\partial \boldsymbol{\sigma}}{\partial t} - \mathbf{E} \cdot \nabla \mathbf{v} = 0,$$
$$\frac{\partial \rho \mathbf{v}}{\partial t} - \nabla \cdot \boldsymbol{\sigma} = 0,$$

$\mathbf{E}$ is the usual stiffness tensor according to the Hooke law $\sigma_{ij} = E_{ijkl}\epsilon_{kl}$

Sharp Interface approach

A high order method on unstructured staggered meshes

Diffuse interface approach

A diffuse interface method on Cartesian AMR grids

Sharp Interface approach

Unstructured staggered mesh

Example

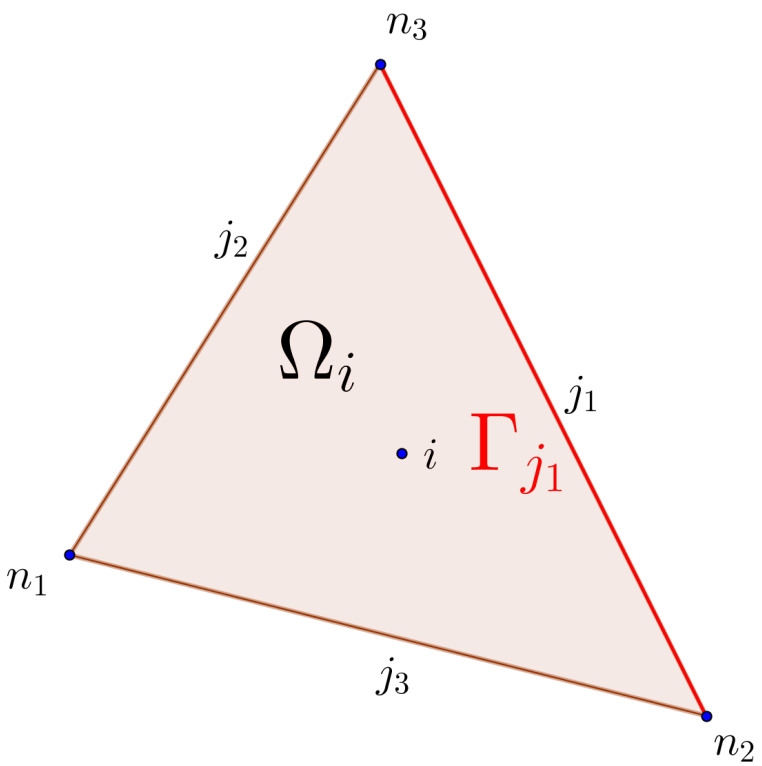

- $\Omega_i = \{n_1, n_2, n_3\}$
- $S_i = \{j_1, j_2, j_3\}$
- $\Gamma_{j_1} = \{n_2, n_3\}$

Example

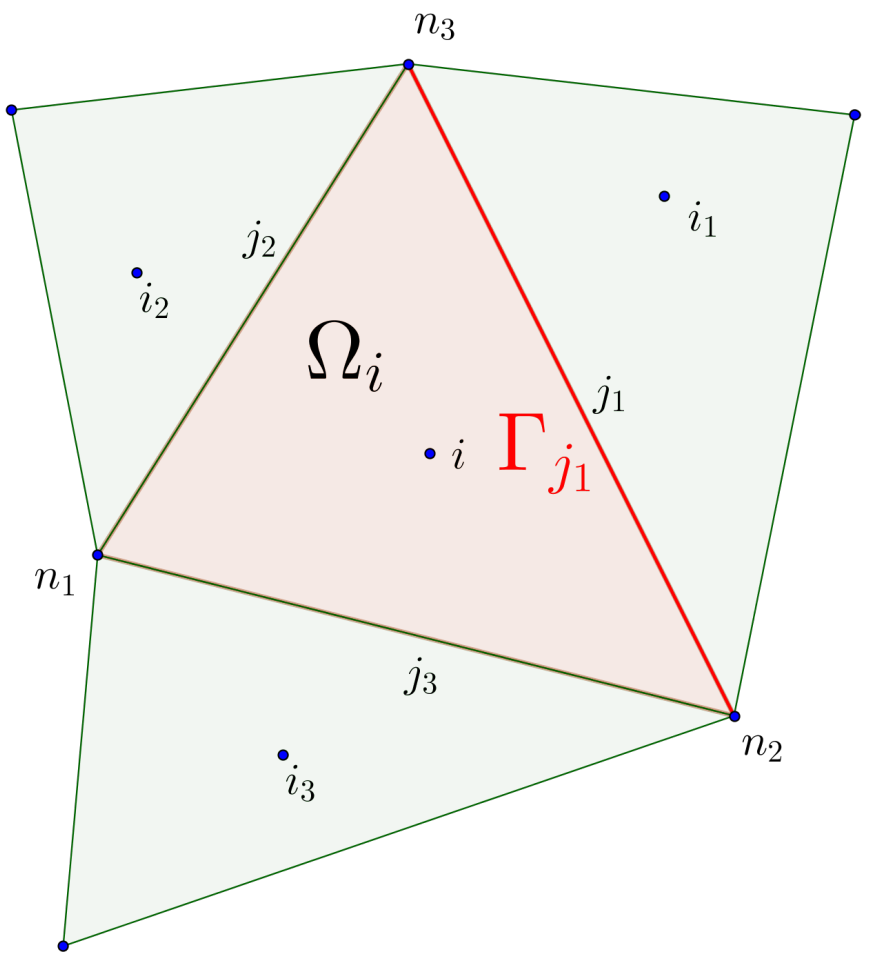

- $\Omega_i = \{n_1, n_2, n_3\}$
- $S_i = \{j_1, j_2, j_3\}$
- $\Gamma_{j_1} = \{n_2, n_3\}$

Example

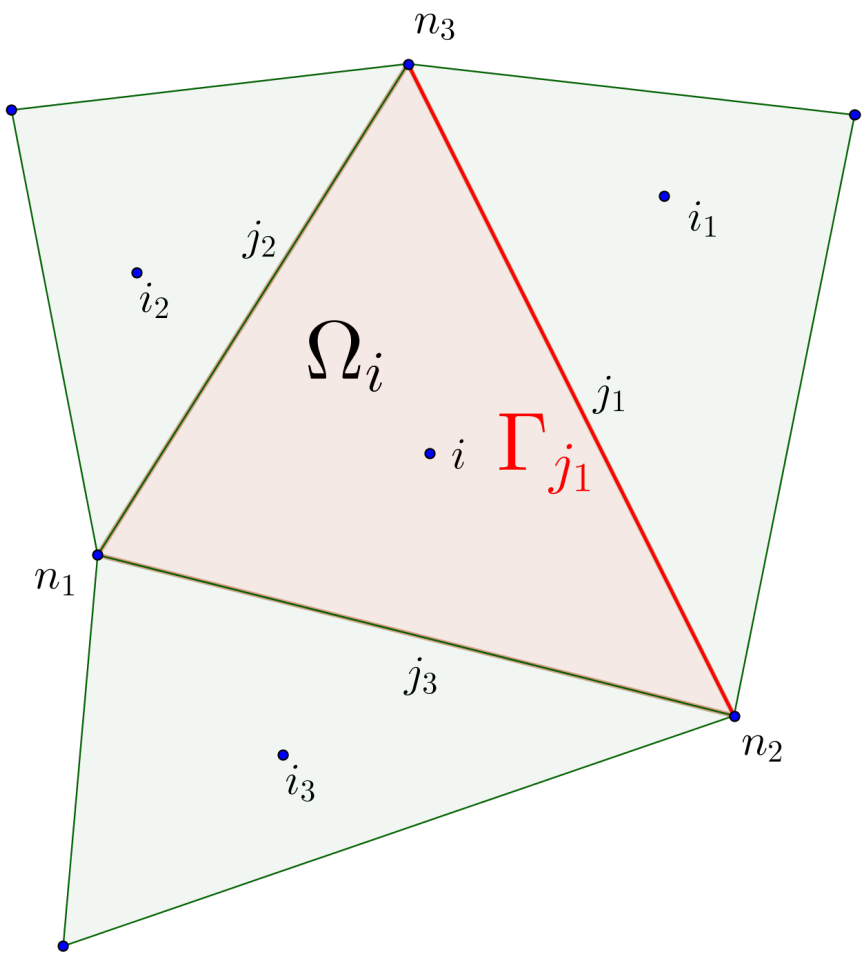

- $\Omega_i = \{n_1, n_2, n_3\}$
- $S_i = \{j_1, j_2, j_3\}$
- $\Gamma_{j_1} = \{n_2, n_3\}$
- $\ell(j_1) = i$ and $r(j_1) = i_1$
- $\wp(i, j_1) = i_1$

Example

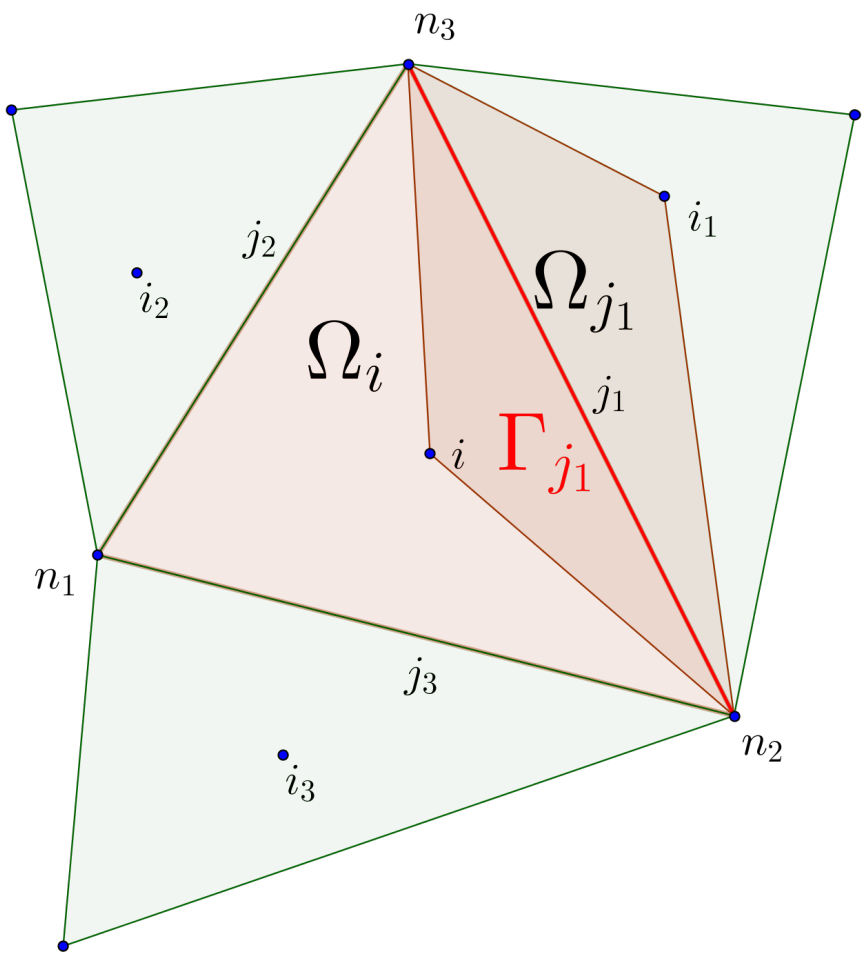

- $\Omega_i = \{n_1, n_2, n_3\}$
- $S_i = \{j_1, j_2, j_3\}$
- $\Gamma_{j_1} = \{n_2, n_3\}$
- $\ell(j_1) = i$ and $r(j_1) = i_1$
- $\wp(i, j_1) = i_1$
- $\Omega_{j_1} = \{i, i_1, \Gamma_{j_1}\}$

Example

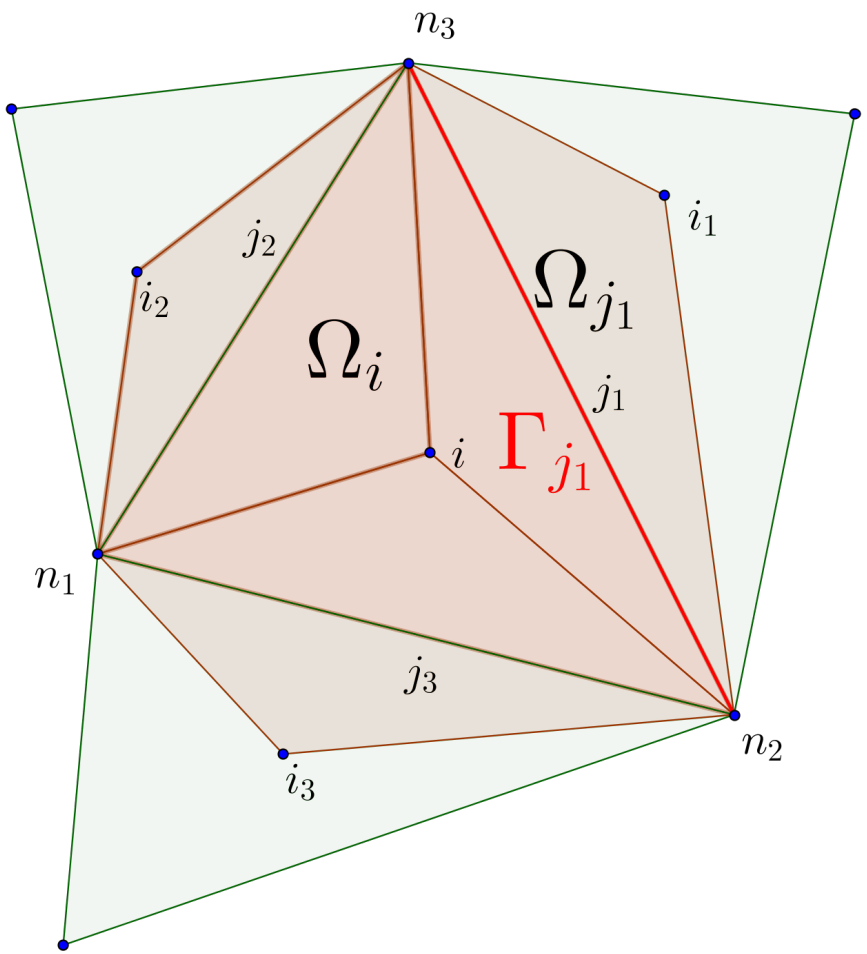

- $\Omega_i = \{n_1, n_2, n_3\}$
- $S_i = \{j_1, j_2, j_3\}$
- $\Gamma_{j_1} = \{n_2, n_3\}$
- $\ell(j_1) = i$ and $r(j_1) = i_1$
- $\wp(i, j_1) = i_1$
- $\Omega_{j_1} = \{i, i_1, \Gamma_{j_1}\}$

Basis Functions

Fixed $p \in \mathbb{N}$ we want a polynomial basis able to reconstruct exactly a polynomial of degree p.
It depends on the element where we want to reconstruct the polynomial.
$\{(\xi_k, \gamma_k)\}_{k=1\ldots N}$ a set of distinct points in the reference element T_{std} or R_{std}, the coefficients of the polynomials can be found by imposing

$$\phi_k(\xi_l, \gamma_l) = \begin{cases} 1 & k = l \\ 0 & k \neq l \end{cases}$$

and solving a linear system.

Basis Functions

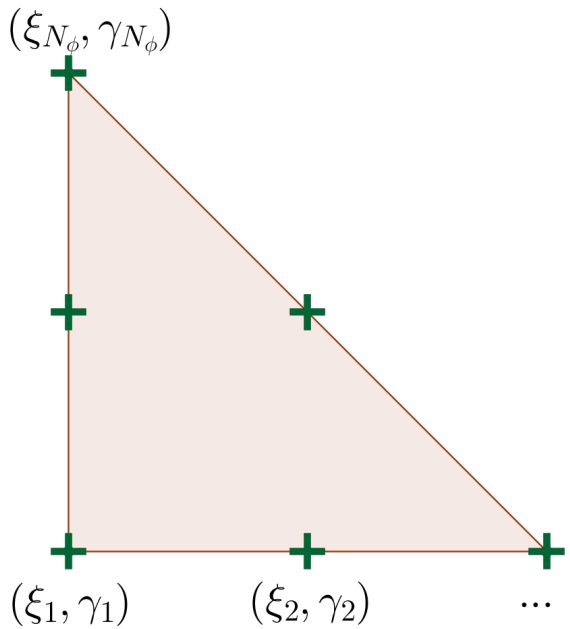

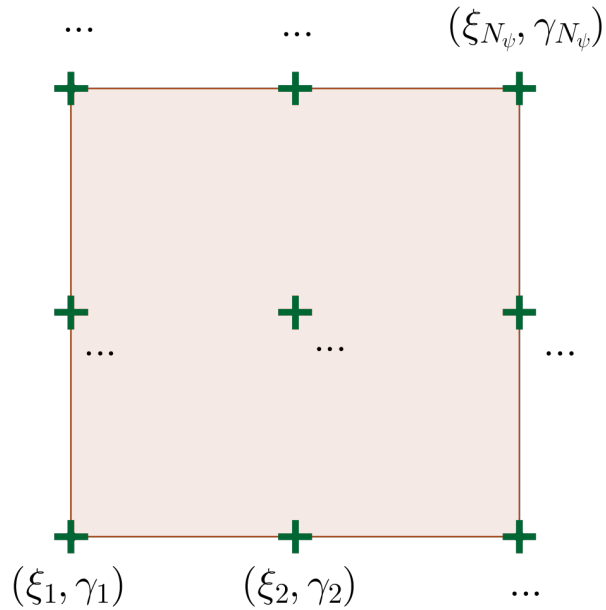

Basis Function $\{\phi_k\}_{k=1...N_\phi}$

$N_\phi = \frac{(p+1)(p+2)}{2}$

Basis Function $\{\psi_k\}_{k=1...N_\psi}$

$N_\psi = (p+1)^2$

Triangle Transformations

$$N_1(\xi,\gamma) = 1-\xi-\gamma \quad ; \quad N_2(\xi,\gamma) = \xi \quad ; \quad N_3(\xi,\gamma) = \gamma$$

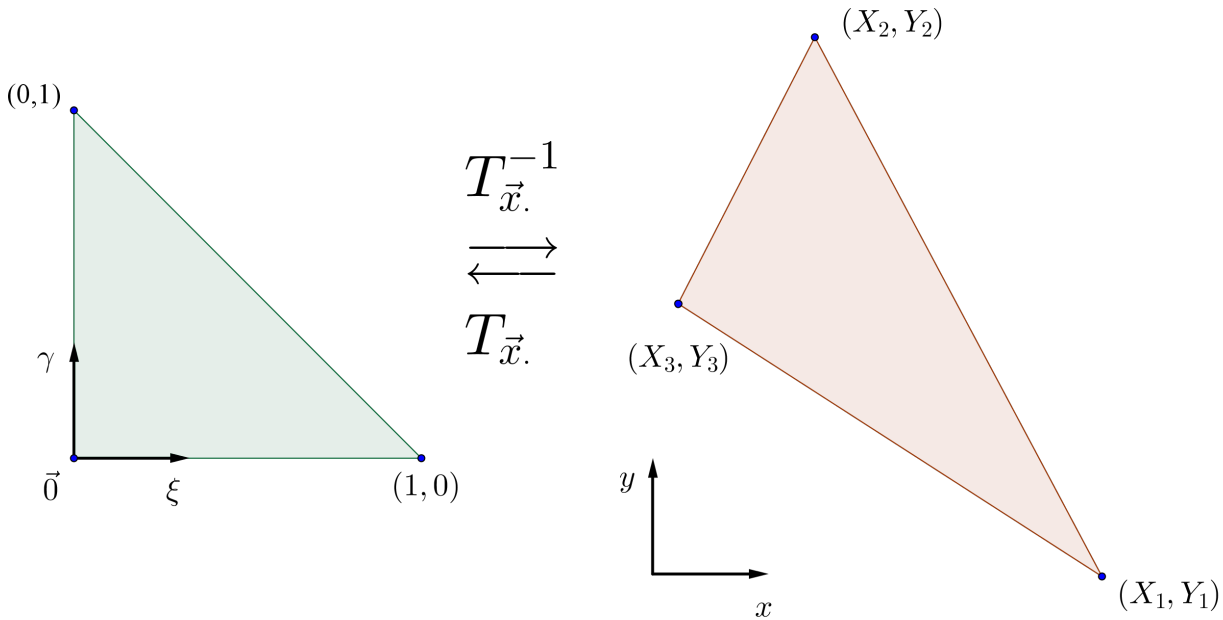

$$(\xi,\gamma) \xrightarrow{T_i^{-1}} \left(x = \sum_{p=1}^{3} N_p X_p, y = \sum_{p=1}^{3} N_p Y_p \right)$$

Triangle Transformations

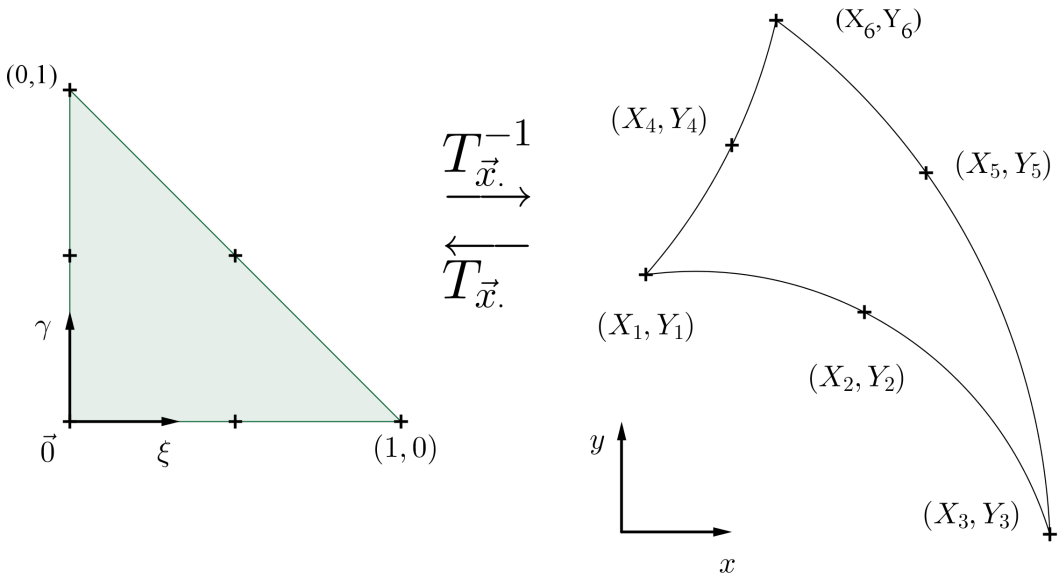

$$(\xi, \gamma) \xrightarrow{T_i^{-1}} \left(x = \sum_{p=1}^{N_\phi} N_p X_p, y = \sum_{p=1}^{N_\phi} N_p Y_p \right)$$

Space-Time extension

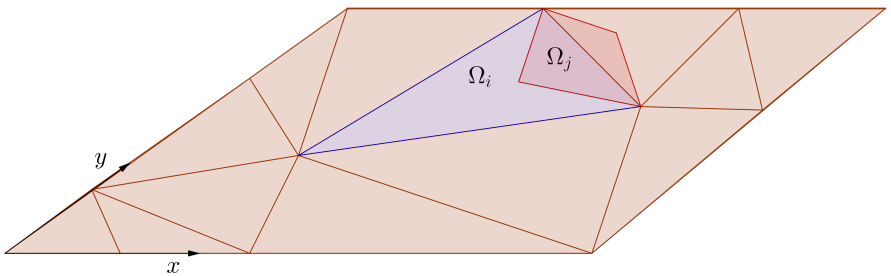

$\Omega_i, \{\phi_k(\mathbf{x})\}, N_\phi = N_\phi(p)$

$\Omega_j, \{\psi_k(\mathbf{x})\}, N_\psi = N_\psi(p)$

Space-Time extension

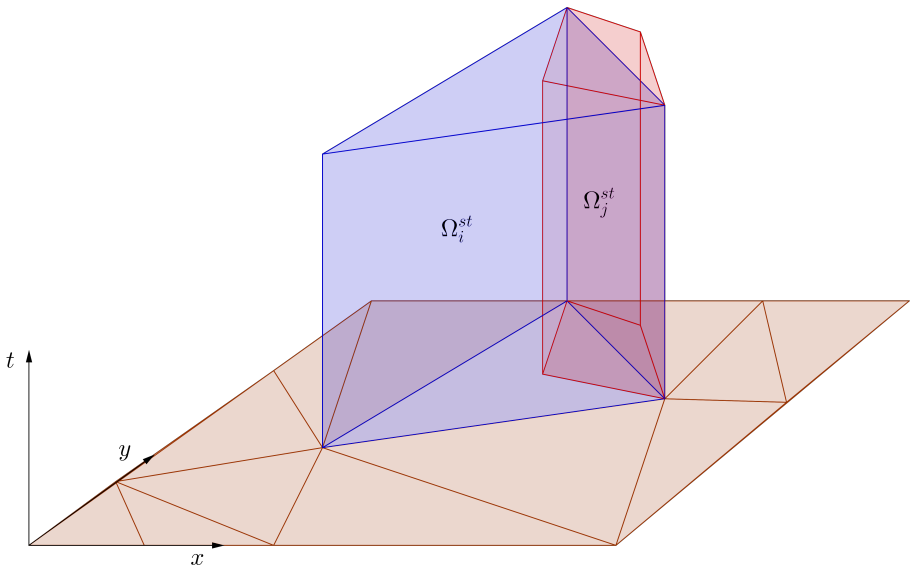

$$\Omega_i, \{\phi_k(\mathbf{x})\}, N_\phi = N_\phi(p) \rightarrow \Omega_i^{st} = \Omega_i \times T, \{\tilde{\phi}_k(\mathbf{x}, t)\}, N_\phi^{st} = N_\phi(p) \cdot (p_\gamma + 1)$$

$$\Omega_j, \{\psi_k(\mathbf{x})\}, N_\psi = N_\psi(p) \rightarrow \Omega_j^{st} = \Omega_j \times T, \{\tilde{\psi}_k(\mathbf{x}, t)\}, N_\psi^{st} = N_\psi(p) \cdot (p_\gamma + 1)$$

Space-Time extension

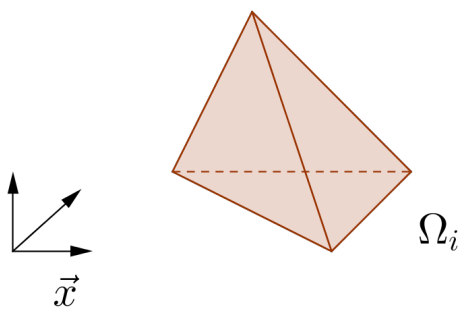

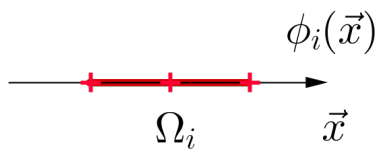

Space-Time extension

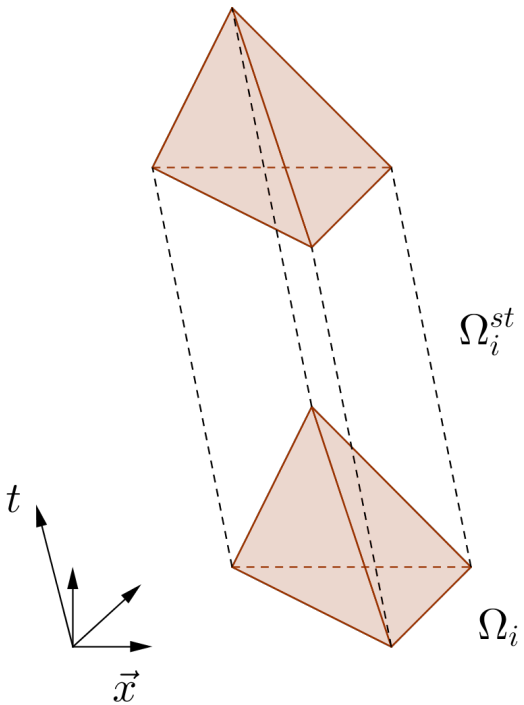

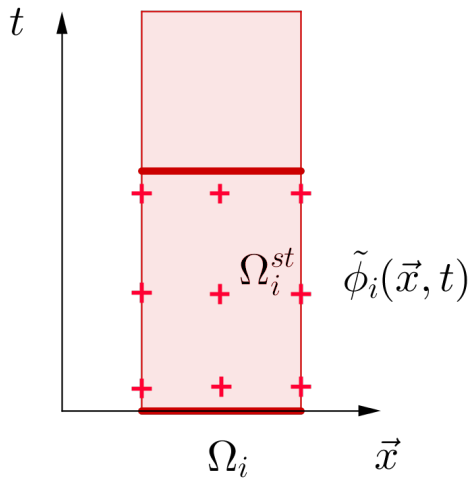

Sharp Interface approach

Numerical method

Definition of the quantities

- $\mathbf{v}_i(\mathbf{x}, t) = \mathbf{v}_h(\mathbf{x}, t)|_{\Omega_i^{st}}$ and $\rho_i(\mathbf{x}) = \rho_h(\mathbf{x})|_{\Omega_i^{st}}$ are defined on the main grid;
- $\boldsymbol{\sigma}_j(\mathbf{x}, t) = \boldsymbol{\sigma}_h(\mathbf{x}, t)|_{\Omega_j^{st}}$ and $\mathbf{E}_j(\mathbf{x}) = \mathbf{E}_h(\mathbf{x})|_{\Omega_j^{st}}$ are defined on the dual grid.

Definition of the quantities

- $\mathbf{v}_i(\mathbf{x},t) = \mathbf{v}_h(\mathbf{x},t)|_{\Omega_i^{st}}$ and $\rho_i(\mathbf{x}) = \rho_h(\mathbf{x})|_{\Omega_i^{st}}$ are defined on the main grid;
- $\boldsymbol{\sigma}_j(\mathbf{x},t) = \boldsymbol{\sigma}_h(\mathbf{x},t)|_{\Omega_j^{st}}$ and $\mathbf{E}_j(\mathbf{x}) = \mathbf{E}_h(\mathbf{x})|_{\Omega_j^{st}}$ are defined on the dual grid.

$$
\begin{aligned}
\mathbf{v}_i(\mathbf{x},t) &= \sum_{l=1}^{N_\phi^{st}} \tilde{\phi}_l^{(i)}(\mathbf{x},t)\hat{\mathbf{v}}_{l,i}^{n+1} =: \tilde{\boldsymbol{\phi}}^{(i)}(\mathbf{x},t)\hat{\mathbf{v}}_i^{n+1}, \\
\rho_i(\mathbf{x},t) &= \sum_{l=1}^{N_\phi^{st}} \tilde{\phi}_l^{(i)}(\mathbf{x},t)\hat{\mathbf{v}}_{l,i}^{n+1} =: \tilde{\boldsymbol{\phi}}^{(i)}(\mathbf{x},t)\hat{\rho}_i^{n+1}, \\
\boldsymbol{\sigma}_j(\mathbf{x},t) &= \sum_{l=1}^{N_\psi^{st}} \tilde{\psi}_l^{(j)}(\mathbf{x},t)\hat{\sigma}_{l,j}^{n+1} =: \tilde{\boldsymbol{\psi}}^{(j)}(\mathbf{x},t)\hat{\boldsymbol{\sigma}}_j^{n+1}, \\
\mathbf{E}_j(\mathbf{x}) &= \sum_{l=1}^{N_\psi^{st}} \tilde{\psi}_l^{(j)}(\mathbf{x})\hat{\mathbf{E}}_{l,j} =: \tilde{\boldsymbol{\psi}}^{(j)}(\mathbf{x})\hat{\mathbf{E}}_j.
\end{aligned}
$$

Weak formulation

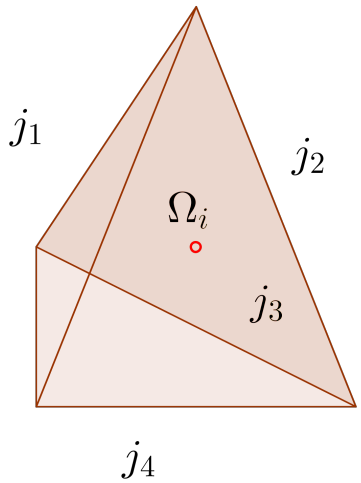

$$\int_{\Omega_i^{st}} \tilde{\phi}_k^{(i)} \frac{\partial \rho \mathbf{v}}{\partial t} d\mathbf{x}\, dt - \int_{\Omega_i^{st}} \tilde{\phi}_k^{(i)} \nabla \cdot \boldsymbol{\sigma}\, d\mathbf{x}\, dt = 0.$$

Weak formulation

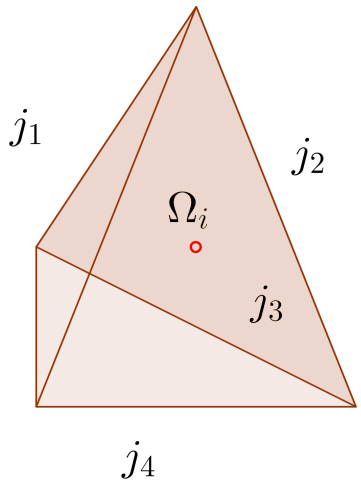

$$\int_{\Omega_i^{st}} \tilde{\phi}_k^{(i)} \frac{\partial \rho \mathbf{v}}{\partial t} d\mathbf{x}\, dt - \left(\int_{\partial\Omega_i^{st}} \tilde{\phi}_k^{(i)} \boldsymbol{\sigma} \cdot \mathbf{n}_i dS\, dt - \int_{\Omega_i^{st}} \nabla \tilde{\phi}_k^{(i)} \cdot \boldsymbol{\sigma} d\mathbf{x}\, dt \right) = 0,$$

Weak formulation

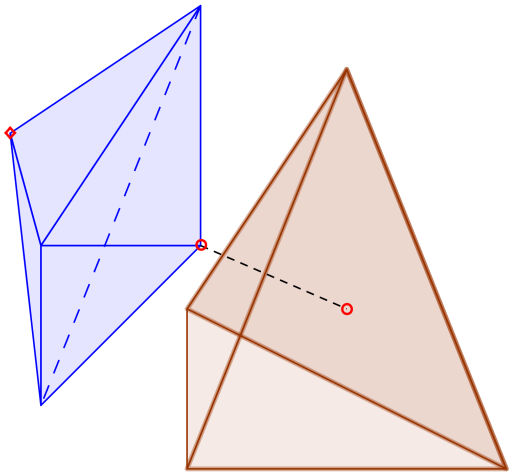

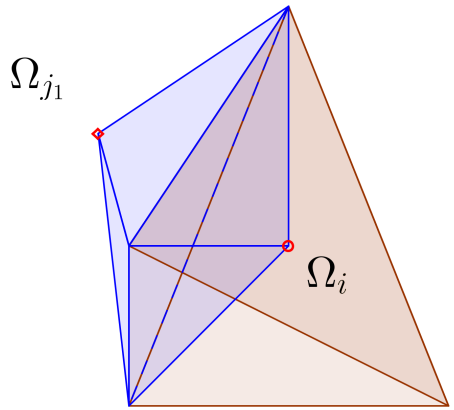

$$\int_{\Omega_i^{st}} \tilde{\phi}_k^{(i)} \frac{\partial \rho \mathbf{v}}{\partial t} d\mathbf{x}\, dt - \left(\int_{\partial\Omega_i^{st}} \tilde{\phi}_k^{(i)} \boldsymbol{\sigma} \cdot \mathbf{n}_i dS\, dt - \int_{\Omega_i^{st}} \nabla \tilde{\phi}_k^{(i)} \cdot \boldsymbol{\sigma} d\mathbf{x}\, dt \right) = 0,$$

Weak formulation

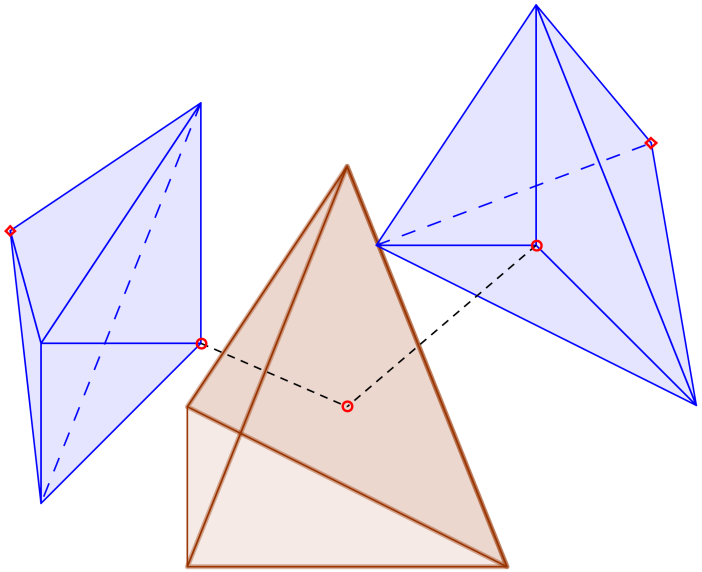

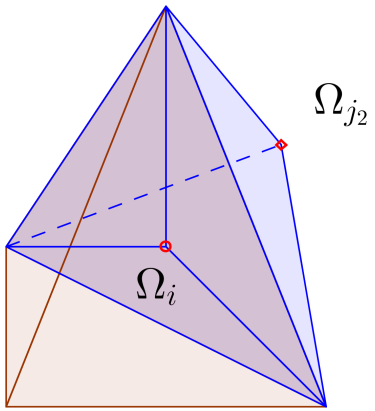

$$\int_{\Omega_i^{st}} \tilde{\phi}_k^{(i)} \frac{\partial \rho \mathbf{v}}{\partial t} d\mathbf{x}\, dt - \left(\int_{\partial\Omega_i^{st}} \tilde{\phi}_k^{(i)} \boldsymbol{\sigma} \cdot \mathbf{n}_i dS\, dt - \int_{\Omega_i^{st}} \nabla \tilde{\phi}_k^{(i)} \cdot \boldsymbol{\sigma}\, d\mathbf{x}\, dt \right) = 0,$$

Weak formulation

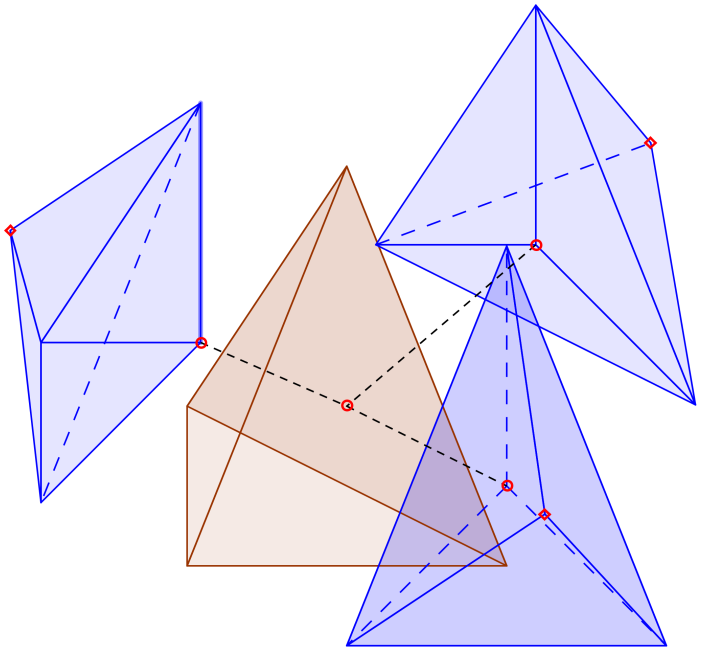

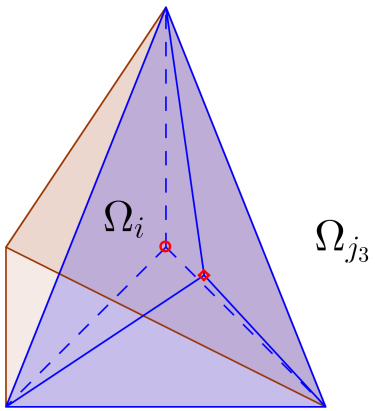

$$\int_{\Omega_i^{st}} \tilde{\phi}_k^{(i)} \frac{\partial \rho \mathbf{v}}{\partial t} d\mathbf{x}\, dt - \left(\int_{\partial\Omega_i^{st}} \tilde{\phi}_k^{(i)} \boldsymbol{\sigma} \cdot \mathbf{n}_i dS\, dt - \int_{\Omega_i^{st}} \nabla \tilde{\phi}_k^{(i)} \cdot \boldsymbol{\sigma}\, d\mathbf{x}\, dt \right) = 0,$$

Weak formulation

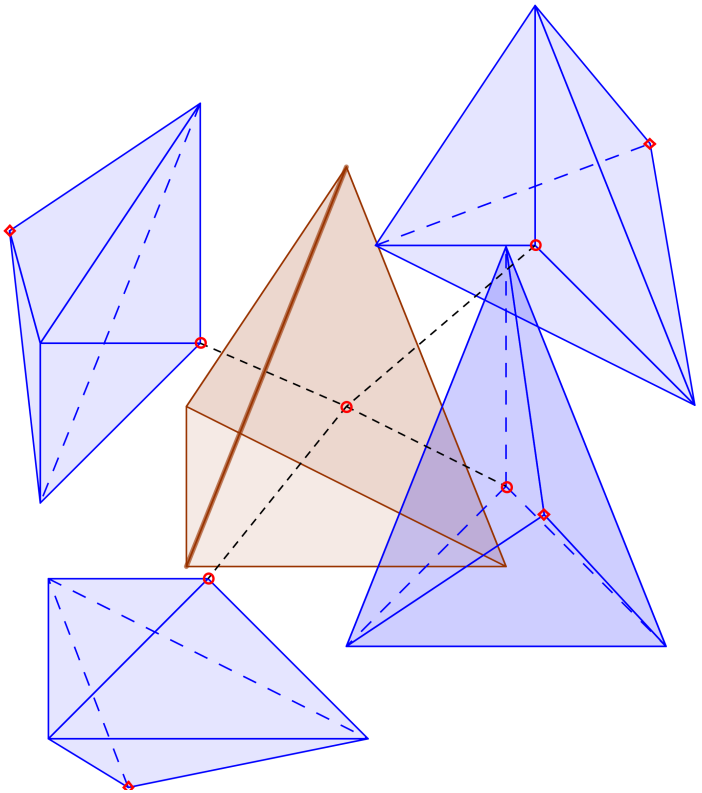

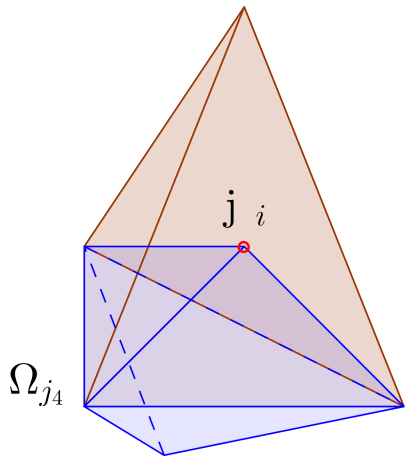

$$\int_{\Omega_i^{st}} \tilde{\phi}_k^{(i)} \frac{\partial \rho \mathbf{v}}{\partial t} d\mathbf{x}\, dt - \left(\int_{\partial\Omega_i^{st}} \tilde{\phi}_k^{(i)} \boldsymbol{\sigma} \cdot \mathbf{n}_i dS\, dt - \int_{\Omega_i^{st}} \nabla \tilde{\phi}_k^{(i)} \cdot \boldsymbol{\sigma}\, d\mathbf{x}\, dt \right) = 0,$$

Weak formulation

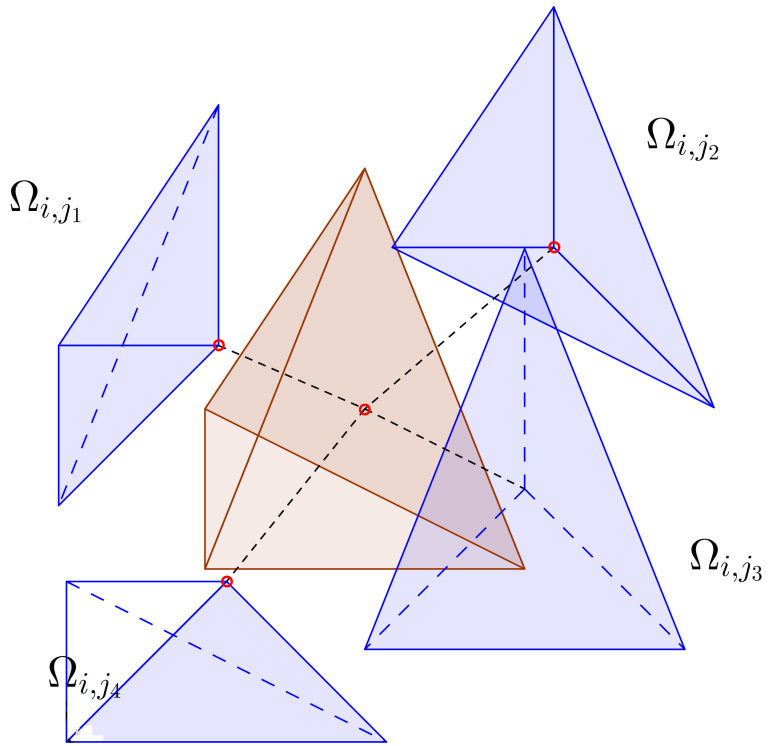

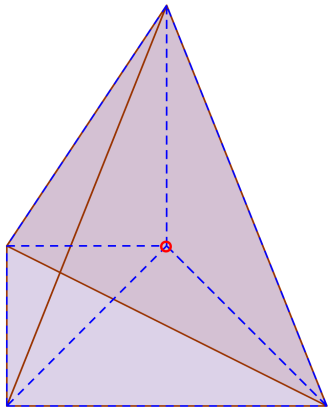

$$\int_{\Omega_i^{st}} \tilde{\phi}_k^{(i)} \frac{\partial (\rho \mathbf{v})_i}{\partial t} d\mathbf{x}\, dt - \sum_{j \in S_i} \left(\int_{\Gamma_j^{st}} \tilde{\phi}_k^{(i)} \boldsymbol{\sigma}_j \cdot \mathbf{n}_{i,j} dS\, dt - \int_{\Omega_{i,j}^{st}} \nabla \tilde{\phi}_k^{(i)} \cdot \boldsymbol{\sigma}_j d\mathbf{x}\, dt \right) = 0,$$

Weak formulation

$$\int_{\Omega_i^{st}} \tilde{\phi}_k^{(i)} \frac{\partial(\rho\mathbf{v})_i}{\partial t}\, d\mathbf{x}\, dt = \int_{\Omega_i} \tilde{\phi}_k^{(i)}(\mathbf{x}, t^{n+1,-})\rho\mathbf{v}_i(\mathbf{x}, t^{n+1,-})d\mathbf{x} - \int_{\Omega_i} \tilde{\phi}_k^{(i)}(\mathbf{x}, t^{n,+})\rho\mathbf{v}_i(\mathbf{x}, t^{n,-})d\mathbf{x}$$

$$- \int_{\Omega_i^{st}} \frac{\partial\tilde{\phi}_k^{(i)}}{\partial t}(\rho\mathbf{v})_i d\mathbf{x}\, dt\,,$$

Weak formulation

$$\int_{\Omega_i^{st}} \tilde{\phi}_k^{(i)} \frac{\partial (\rho \mathbf{v})_i}{\partial t} \, d\mathbf{x}\, dt = \int_{\Omega_i} \tilde{\phi}_k^{(i)}(\mathbf{x}, t^{n+1,-}) \rho \mathbf{v}_i(\mathbf{x}, t^{n+1,-}) d\mathbf{x} - \int_{\Omega_i} \tilde{\phi}_k^{(i)}(\mathbf{x}, t^{n,+}) \rho \mathbf{v}_i(\mathbf{x}, t^{n,-}) d\mathbf{x} - \int_{\Omega_i^{st}} \frac{\partial \tilde{\phi}_k^{(i)}}{\partial t} (\rho \mathbf{v})_i \, d\mathbf{x}\, dt \,,$$

$$\Downarrow$$

$$\left(\int_{\Omega_i} \tilde{\phi}_k^{(i)}(\mathbf{x}, t^{n+1,-}) \tilde{\phi}_m^{(i)}(\mathbf{x}, t^{n+1,-}) d\mathbf{x} - \int_{\Omega_i^{st}} \frac{\partial \tilde{\phi}_k^{(i)}}{\partial t} \tilde{\phi}_m^{(i)} \, d\mathbf{x}\, dt \right) (\hat{\rho \mathbf{v}})_{m,i}^{n+1} - \int_{\Omega_i} \tilde{\phi}_k^{(i)}(\mathbf{x}, t^{n,+}) \tilde{\phi}_m^{(i)}(\mathbf{x}, t^{n,-}) d\mathbf{x} \, (\hat{\rho \mathbf{v}})_{m,i}^{n}$$
$$- \sum_{j \in S_i} \left(\int_{\Gamma_j^{st}} \tilde{\phi}_k^{(i)} \tilde{\psi}_m^{(j)} \mathbf{n}_{i,j} dS \, dt - \int_{\Omega_{i,j}^{st}} \nabla \tilde{\phi}_k^{(i)} \tilde{\psi}_m^{(j)} \, d\mathbf{x}\, dt \right) \cdot \hat{\boldsymbol{\sigma}}_{m,j}^{n+1} = 0$$

$$\Downarrow$$

$$\bar{\boldsymbol{M}}_i (\hat{\rho \mathbf{v}})_i^{n+1} = \bar{\boldsymbol{M}}_i^{-} (\hat{\rho \mathbf{v}})_i^{n} + \sum_{j \in S_i} \boldsymbol{\mathcal{D}}_{i,j} \cdot \hat{\boldsymbol{\sigma}}_j^{n+1},$$

Weak formulation

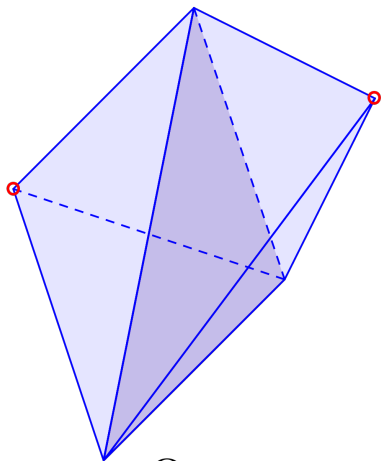

$$\int_{\Omega_j^{st}} \tilde{\psi}_k^{(j)} \frac{\partial \boldsymbol{\sigma}}{\partial t} d\mathbf{x}\, dt \; - \int_{\Omega_j^{st}} \tilde{\psi}_k^{(j)} \mathbf{E} \cdot \nabla \mathbf{v} d\mathbf{x}\, dt \; = 0.$$

Weak formulation

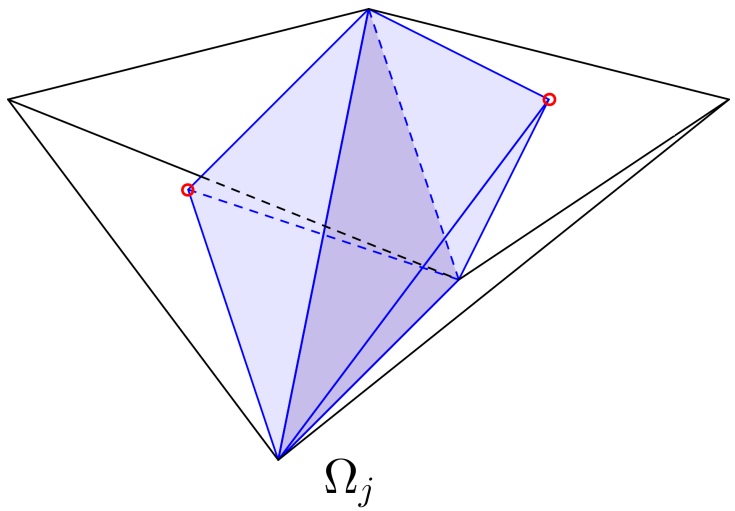

$$\int_{\Omega_j^{st}} \tilde{\psi}_k^{(j)} \frac{\partial \boldsymbol{\sigma}}{\partial t} d\mathbf{x}\, dt \; - \int_{\Omega_j^{st}} \tilde{\psi}_k^{(j)} \mathbf{E} \cdot \nabla \mathbf{v} d\mathbf{x}\, dt \; = 0.$$

Weak formulation

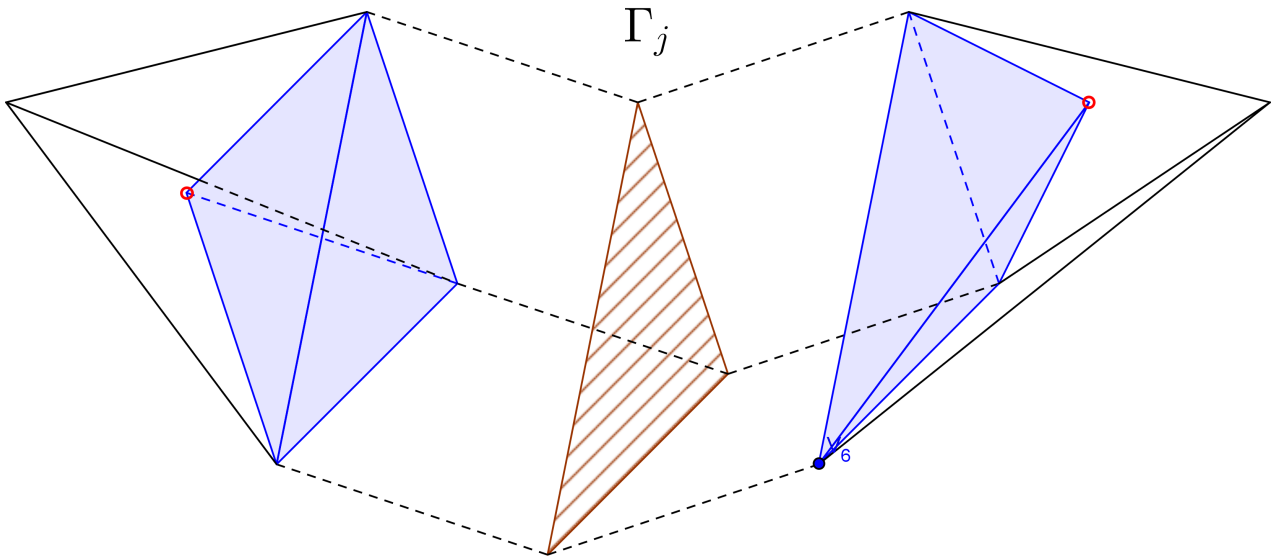

$$\int_{\Omega_j^{st}} \tilde{\psi}_k^{(j)} \frac{\partial \boldsymbol{\sigma}_j}{\partial t} d\mathbf{x}\, dt - \int_{\Omega_{\ell(j),j}^{st}} \tilde{\psi}_k^{(j)} \mathbf{E}_j \cdot \nabla \mathbf{v}_{\ell(j)} d\mathbf{x}\, dt - \int_{\Omega_{r(j),j}^{st}} \tilde{\psi}_k^{(j)} \mathbf{E}_j \cdot \nabla \mathbf{v}_{r(j)} d\mathbf{x}\, dt - \int_{\Gamma_j^{st}} \tilde{\psi}_k^{(j)} \mathbf{E}_j \cdot (\mathbf{v}_{r(j)} - \mathbf{v}_{\ell(j)}) \otimes \mathbf{n}_j dS\, dt = 0.$$

Weak formulation

$$\left(\int_{\Omega_j} \tilde{\psi}_k^{(i)}(\mathbf{x}, t^{n+1,-}) \tilde{\psi}_m^{(i)}(\mathbf{x}, t^{n+1,-}) d\mathbf{x} \; - \int_{\Omega_j^{st}} \frac{\partial \tilde{\psi}_k^{(i)}}{\partial t} \tilde{\psi}_m^{(i)} d\mathbf{x}\, dt \right) \hat{\boldsymbol{\sigma}}_{m,j}^{n+1} - \int_{\Omega_i} \tilde{\psi}_k^{(i)}(\mathbf{x}, t^{n,+}) \tilde{\psi}_m^{(i)}(\mathbf{x}, t^{n,-}) d\mathbf{x}\, \hat{\boldsymbol{\sigma}}_{m,j}^{n}$$

$$-\hat{\mathbf{E}}_{q,j} \cdot \left(\int_{\Omega_{\ell(j),j}^{st}} \tilde{\psi}_k^{(j)} \nabla \tilde{\phi}_m^{(\ell(j))} \tilde{\psi}_q^{(j)} d\mathbf{x}\, dt \; - \int_{\Gamma_j^{st}} \tilde{\psi}_k^{(j)} \tilde{\phi}_m^{(\ell(j))} \tilde{\psi}_q^{(j)} \mathbf{n}_j dS dt \right) \hat{\mathbf{v}}_{m,\ell(j)}^{n+1}$$

$$-\hat{\mathbf{E}}_{q,j} \cdot \left(\int_{\Omega_{r(j),j}^{st}} \tilde{\psi}_k^{(j)} \nabla \tilde{\phi}_m^{(r(j))} \tilde{\psi}_q^{(j)} d\mathbf{x}\, dt \; + \int_{\Gamma_j^{st}} \tilde{\psi}_k^{(j)} \tilde{\phi}_m^{(r(j))} \tilde{\psi}_q^{(j)} \mathbf{n}_j dS dt \right) \hat{\mathbf{v}}_{m,r(j)}^{n+1} = 0.$$

$$\Downarrow$$

$$\boldsymbol{M}_j \hat{\boldsymbol{\sigma}}_j^{n+1} = \boldsymbol{M}_j^{-} \hat{\boldsymbol{\sigma}}_j^{n} + \hat{\mathbf{E}}_j \cdot \mathcal{Q}_{\ell(j),j} \hat{\mathbf{v}}_{\ell(j)}^{n+1} + \hat{\mathbf{E}}_j \cdot \mathcal{Q}_{r(j),j} \hat{\mathbf{v}}_{r(j)}^{n+1}.$$

Numerical Method

$$\begin{cases} \bar{\boldsymbol{M}}_i(\hat{\rho\mathbf{v}})_i^{n+1} = \bar{\boldsymbol{M}}_i^{-}(\hat{\rho\mathbf{v}})_i^{n} + \sum_{j\in S_i} \boldsymbol{\mathcal{D}}_{i,j}\cdot\hat{\boldsymbol{\sigma}}_j, \\ \boldsymbol{M}_j\hat{\boldsymbol{\sigma}}_j^{n+1} = \boldsymbol{M}_j^{-}\hat{\boldsymbol{\sigma}}_j^{n} + \hat{\mathbf{E}}_j\cdot\boldsymbol{\mathcal{Q}}_{\ell(j),j}\hat{\mathbf{v}}_{\ell(j)} + \hat{\mathbf{E}}_j\cdot\boldsymbol{\mathcal{Q}}_{r(j),j}\hat{\mathbf{v}}_{r(j)} \end{cases}$$

Numerical Method

We get for every i and $j \in S_i$

$$\begin{cases} \bar{\boldsymbol{M}}_i(\hat{\rho\mathbf{v}})_i^{n+1} = \bar{\boldsymbol{M}}_i^-(\hat{\rho\mathbf{v}})_i^n + \sum_{j\in S_i} \mathcal{D}_{i,j} \cdot \hat{\boldsymbol{\sigma}}^{n+1}{}_j, \\ \boldsymbol{M}_j \hat{\boldsymbol{\sigma}}_j^{n+1} = \boldsymbol{M}_j^- \hat{\boldsymbol{\sigma}}_j^n + \hat{\mathbf{E}}_j \cdot \mathcal{Q}_{\ell(j),j} \hat{\mathbf{v}}_{\ell(j)}^{n+1} + \hat{\mathbf{E}}_j \cdot \mathcal{Q}_{r(j),j} \hat{\mathbf{v}}_{r(j)}^{n+1} \end{cases}$$

Numerical Method

Formal substitution of $\hat{\sigma}_j$ in the momentum equation we get

$$\bar{M}_i\,\hat{\rho}_i\hat{\mathbf{v}}_i^{n+1} - \sum_{j\in S_i}\mathcal{D}_{i,j}\cdot M_j^{-1}\left(\hat{\mathbf{E}}_j\cdot\mathcal{Q}_{\ell(j),j}\hat{\mathbf{v}}_{\ell(j)}^{n+1} + \hat{\mathbf{E}}_j\cdot\mathcal{Q}_{r(j),j}\hat{\mathbf{v}}_{r(j)}^{n+1}\right) = \bar{M}_i^-\,\hat{\rho}_i\hat{\mathbf{v}}_i^n + \sum_{j\in S_i}\mathcal{D}_{i,j}\cdot M_j^{-1}M_j^-\,\hat{\sigma}_j^n$$

Numerical Method

Formal substitution of $\hat{\boldsymbol{\sigma}}_j$ in the momentum equation we get

$$\bar{\boldsymbol{M}}_i\, \hat{\rho}_i \hat{\mathbf{v}}_i^{n+1} - \sum_{j \in S_i} \boldsymbol{\mathcal{D}}_{i,j} \cdot \boldsymbol{M}_j^{-1} \left(\hat{\mathbf{E}}_j \cdot \boldsymbol{\mathcal{Q}}_{\ell(j),j} \hat{\mathbf{v}}_{\ell(j)}^{n+1} + \hat{\mathbf{E}}_j \cdot \boldsymbol{\mathcal{Q}}_{r(j),j} \hat{\mathbf{v}}_{r(j)}^{n+1} \right) =$$

$$\bar{\boldsymbol{M}}_i^{-}\, \hat{\rho}_i \hat{\mathbf{v}}_i^{n} + \sum_{j \in S_i} \boldsymbol{\mathcal{D}}_{i,j} \cdot \boldsymbol{M}_j^{-1} \boldsymbol{M}_j^{-}\, \hat{\boldsymbol{\sigma}}_j^{n}$$

- is a 5-points block system in $3D$ and a 4-points block system in $2D$

Numerical Method

Formal substitution of $\hat{\sigma}_j$ in the momentum equation we get

$$\bar{\boldsymbol{M}}_i\,\hat{\rho}_i\hat{\mathbf{v}}_i^{n+1} - \sum_{j\in S_i}\boldsymbol{\mathcal{D}}_{i,j}\cdot\boldsymbol{M}_j^{-1}\left(\hat{\mathbf{E}}_j\cdot\boldsymbol{\mathcal{Q}}_{\ell(j),j}\hat{\mathbf{v}}_{\ell(j)}^{n+1} + \hat{\mathbf{E}}_j\cdot\boldsymbol{\mathcal{Q}}_{r(j),j}\hat{\mathbf{v}}_{r(j)}^{n+1}\right) = \bar{\boldsymbol{M}}_i^{-}\,\hat{\rho}_i\hat{\mathbf{v}}_i^{n} + \sum_{j\in S_i}\boldsymbol{\mathcal{D}}_{i,j}\cdot\boldsymbol{M}_j^{-1}\boldsymbol{M}_j^{-}\,\hat{\boldsymbol{\sigma}}_j^{n}$$

- is a 5-points block system in $3D$ and a 4-points block system in $2D$
- for $p_\gamma = 0$ and homogeneous material is symmetric and positive definite

Numerical Method

Formal substitution of $\hat{\sigma}_j$ in the momentum equation we get

$$\bar{\boldsymbol{M}}_i\, \hat{\rho}_i \hat{\mathbf{v}}_i^{n+1} - \sum_{j \in S_i} \boldsymbol{\mathcal{D}}_{i,j} \cdot \boldsymbol{M}_j^{-1} \left(\hat{\mathbf{E}}_j \cdot \boldsymbol{\mathcal{Q}}_{\ell(j),j} \hat{\mathbf{v}}_{\ell(j)}^{n+1} + \hat{\mathbf{E}}_j \cdot \boldsymbol{\mathcal{Q}}_{r(j),j} \hat{\mathbf{v}}_{r(j)}^{n+1} \right) =$$

$$\bar{\boldsymbol{M}}_i^{-}\, \hat{\rho}_i \hat{\mathbf{v}}_i^{n} + \sum_{j \in S_i} \boldsymbol{\mathcal{D}}_{i,j} \cdot \boldsymbol{M}_j^{-1} \boldsymbol{M}_j^{-}\, \hat{\boldsymbol{\sigma}}_j^{n}$$

- is a 5-points block system in $3D$ and a 4-points block system in $2D$
- for $p_\gamma = 0$ and homogeneous material is symmetric and positive definite
- All the matrices $\boldsymbol{M}, \boldsymbol{\mathcal{Q}}, \boldsymbol{\mathcal{D}}$ can be pre-computed $\forall i,\, j \in S_i$

It can be efficiently solved by the GMRES algorithm or better by the CG Method.

Numerical Method

Further properties of the staggered space-time DG schemes for linear elasticity in the homogeneous case:

- For any $p \geq 0$ $p_\gamma \geq 0$ the fully discrete method is energy stable
- For $p \geq 0$, $p_\gamma = 0$ and for the special case of a Crank-Nicolson time discretization the scheme is also exactly *energy preserving*

Sharp Interface approach

Numerical experiments

Numerical experiments

p	N_i	u		v		σ_{xx}		σ_{yy}	
1	1760	1.253E-01		2.675E-01		5.111E-01		3.003E-01	
1	3960	4.609E-02	2.5	1.284E-01	1.8	2.428E-01	1.8	1.248E-01	2.2
1	7040	2.479E-02	2.2	7.356E-02	1.9	1.387E-01	1.9	6.938E-02	2.0
1	11000	1.567E-02	2.1	4.741E-02	2.0	8.931E-02	2.0	4.430E-02	2.0
p	N_i	u		v		σ_{xx}		σ_{yy}	
2	1760	1.512E-03		3.249E-03		6.081E-03		3.156E-03	
2	3960	3.697E-04	3.5	6.568E-04	3.9	1.218E-03	4.0	6.411E-04	3.9
2	7040	1.416E-04	3.3	2.118E-04	3.9	3.882E-04	4.0	2.086E-04	3.9
2	11000	6.901E-05	3.2	8.872E-05	3.9	1.601E-04	4.0	8.835E-05	3.9
p	N_i	u		v		σ_{xx}		σ_{yy}	
3	1760	5.522E-05		3.323E-05		4.781E-05		3.835E-05	
3	3960	1.079E-05	4.0	5.544E-06	4.4	6.534E-06	4.9	6.313E-06	4.4
3	7040	3.414E-06	4.0	1.677E-06	4.2	1.824E-06	4.4	1.906E-06	4.2
3	11000	1.396E-06	4.0	6.827E-07	4.0	7.183E-07	4.2	7.668E-07	4.1
p	N_i	u		v		σ_{xx}		σ_{yy}	
4	1760	2.480E-06		1.216E-06		1.400E-06		1.434E-06	
4	3960	3.270E-07	5.0	1.582E-07	5.0	1.820E-07	5.0	1.869E-07	5.0
4	7040	7.724E-08	5.0	3.733E-08	5.0	4.292E-08	5.0	4.418E-08	5.0
4	11000	2.532E-08	5.0	1.218E-08	5.0	1.402E-08	5.0	1.442E-08	5.0

Numerical experiments

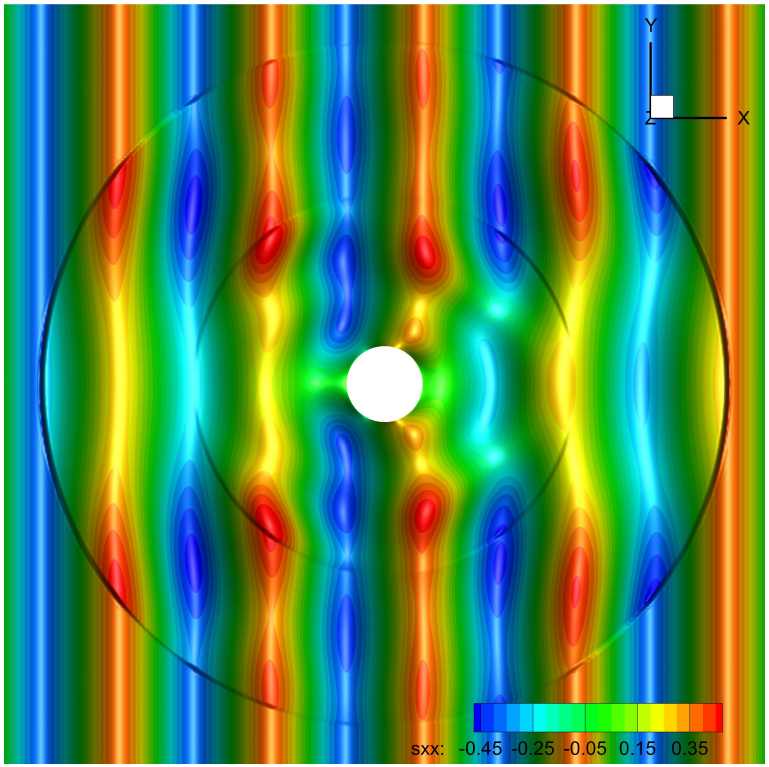

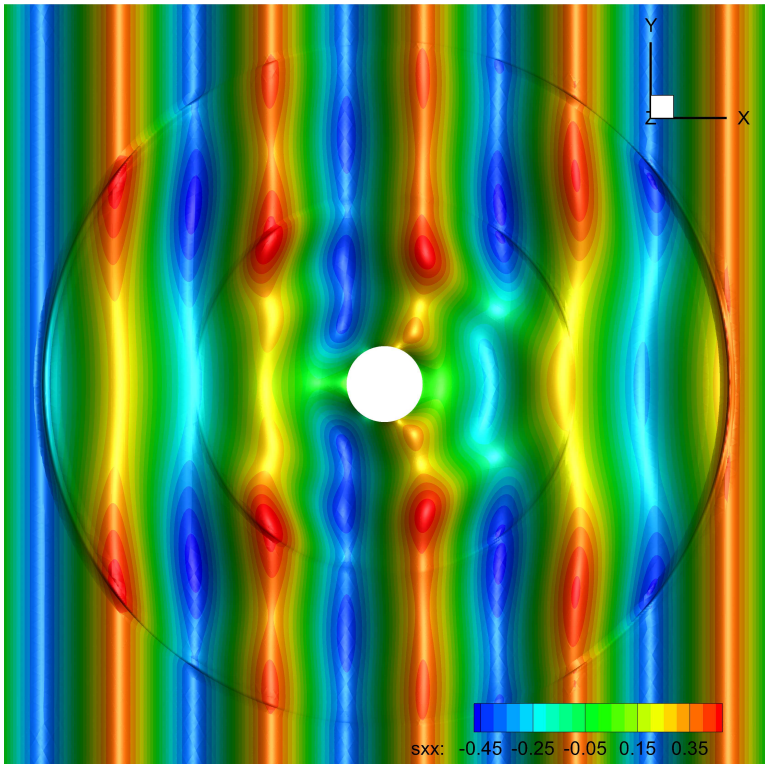

Plane wave scattering on a circular cavity. Comparison of the isocontours of the stress tensor component σ_{xx} between the reference solution given by an explicit ADER-DG scheme (left) and our new staggered space-time DG scheme (right).

Numerical experiments

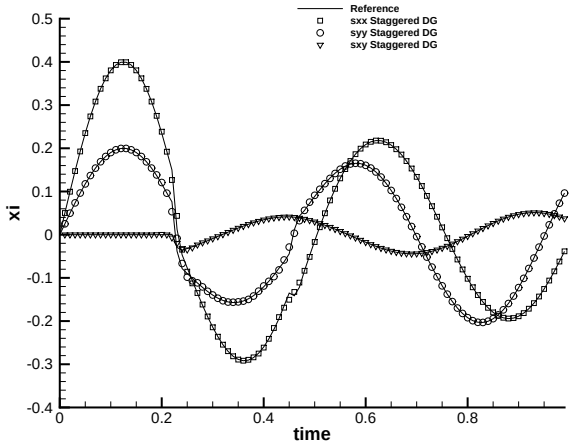

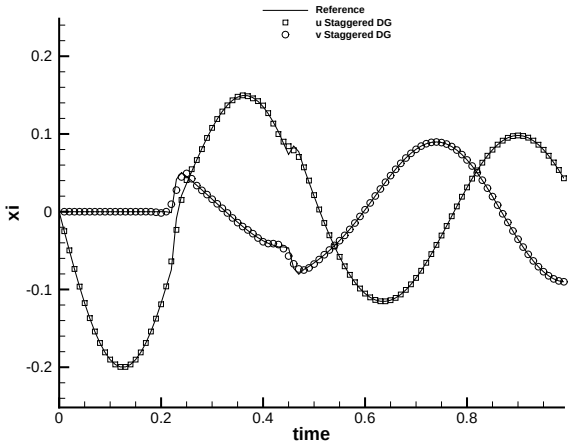

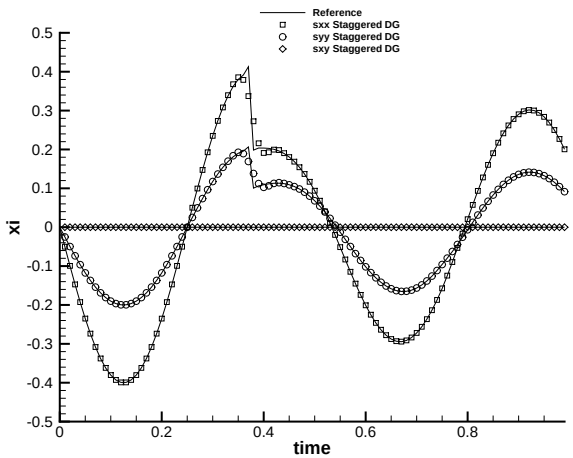

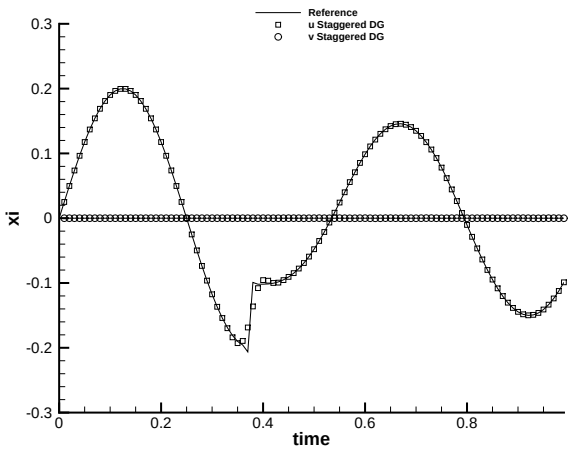

Numerical experiments

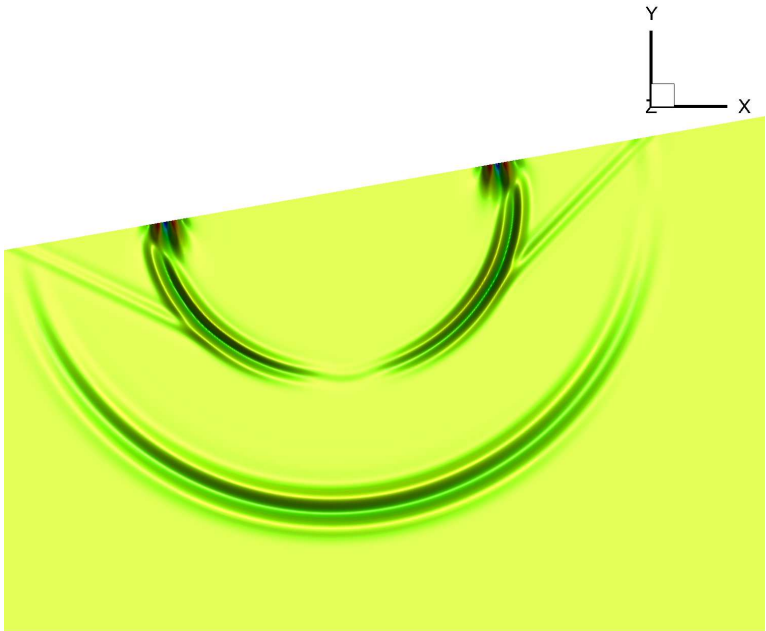

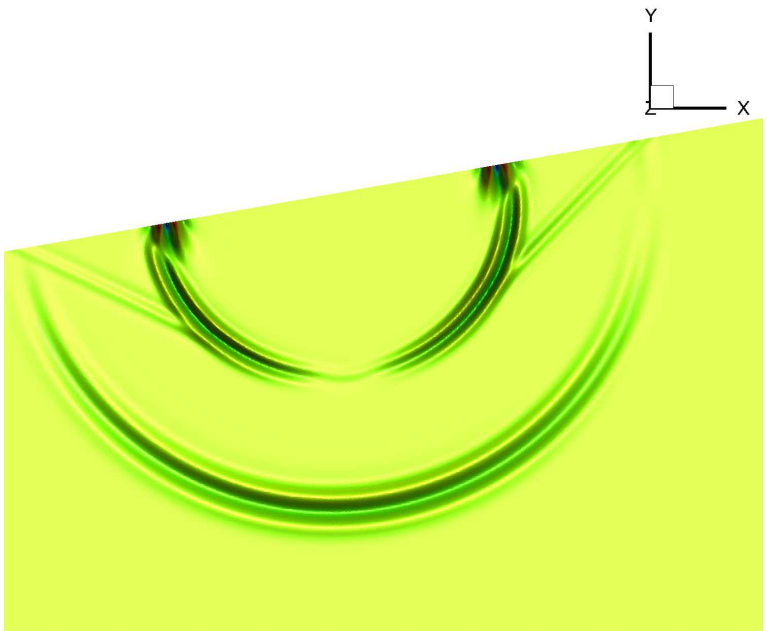

Numerical experiments

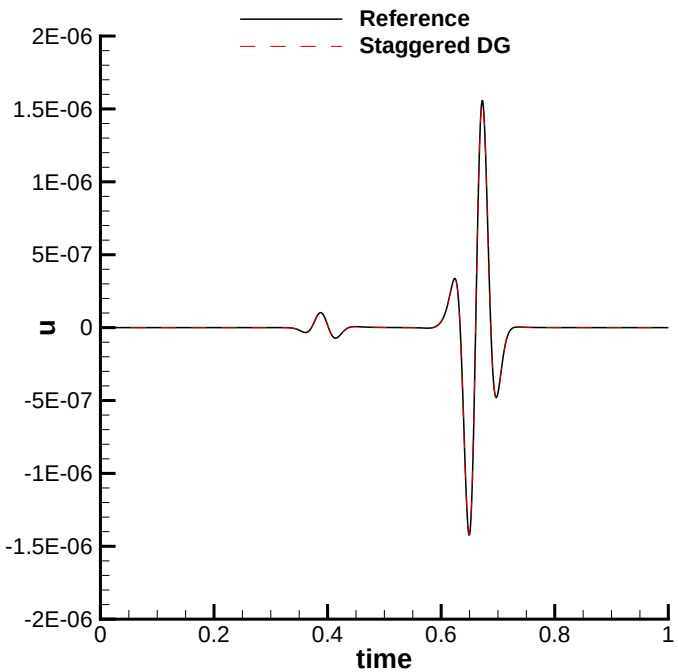

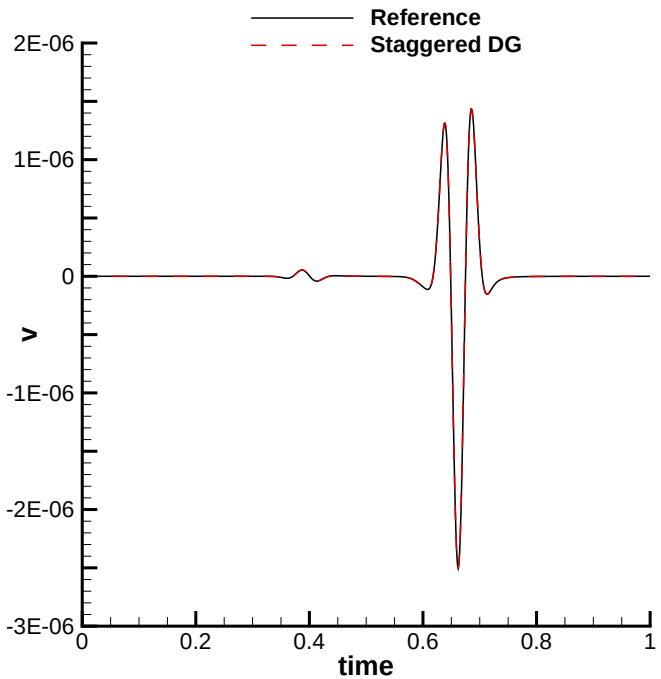

Numerical experiments

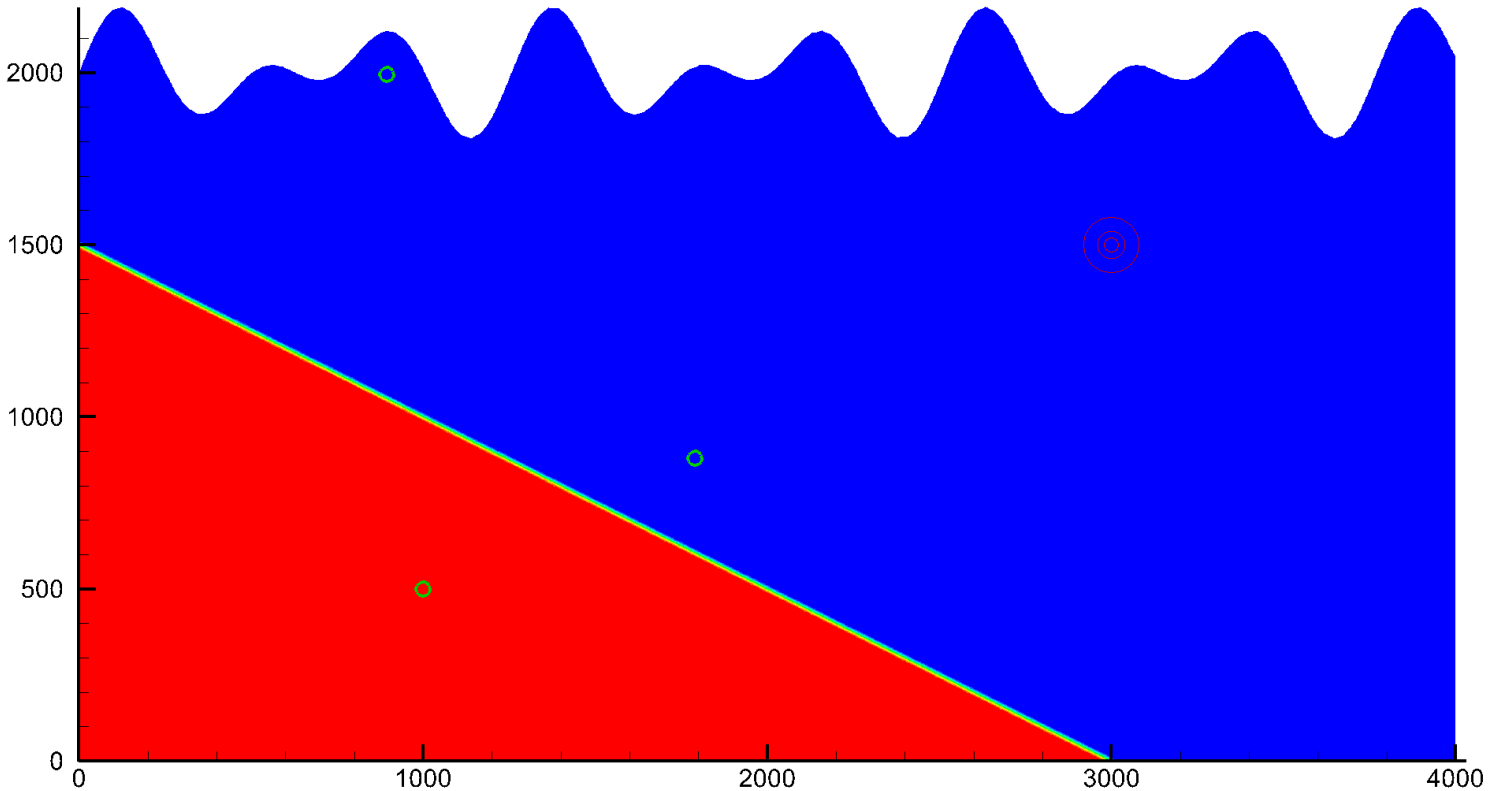

Numerical experiments

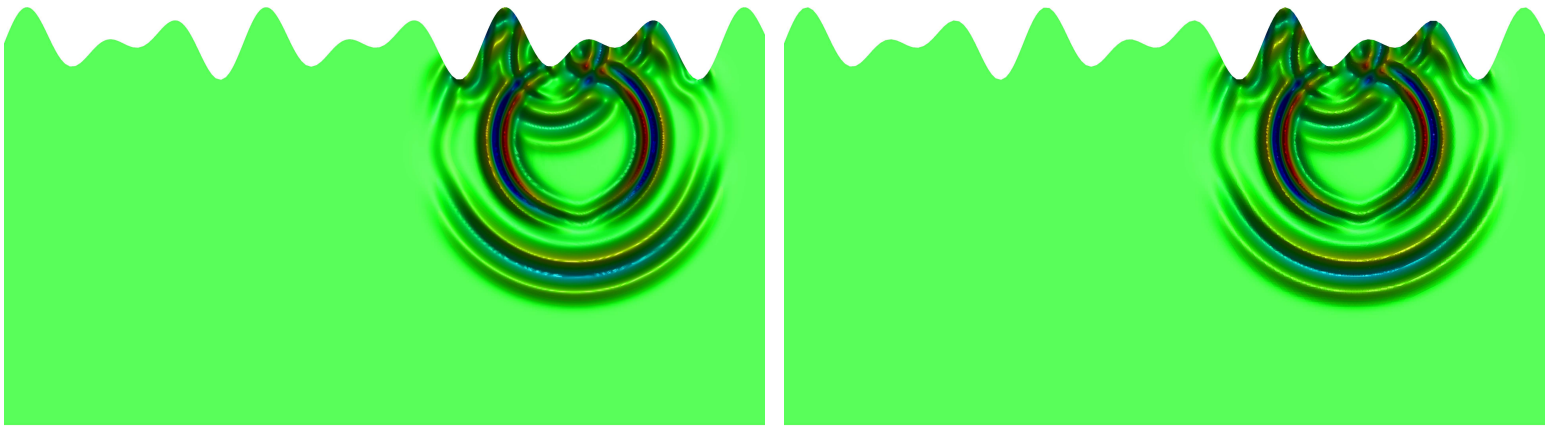

Numerical experiments

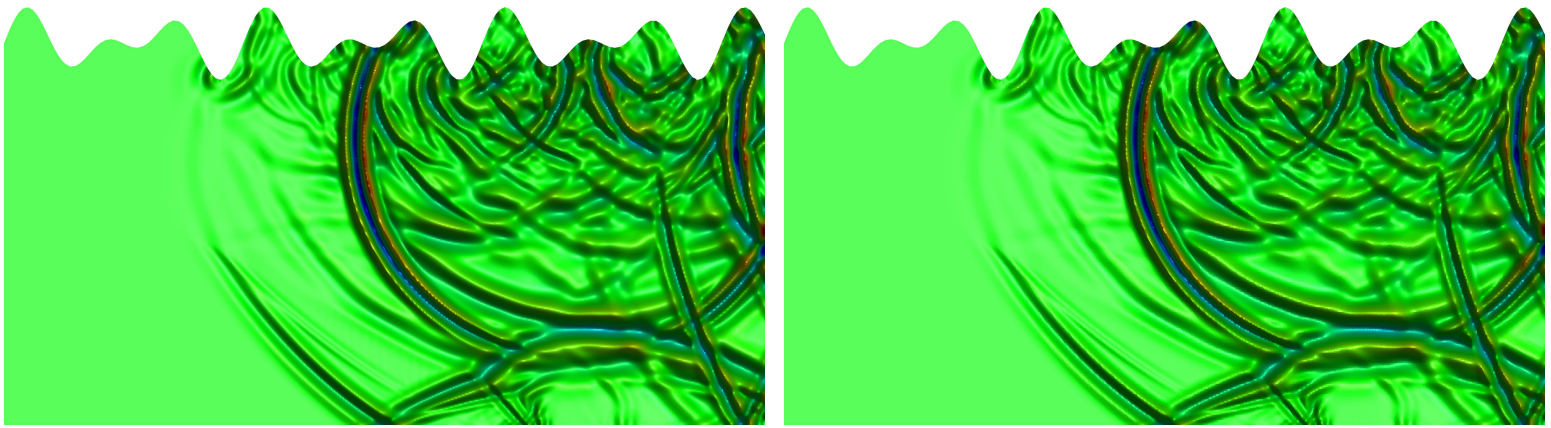

Numerical experiments

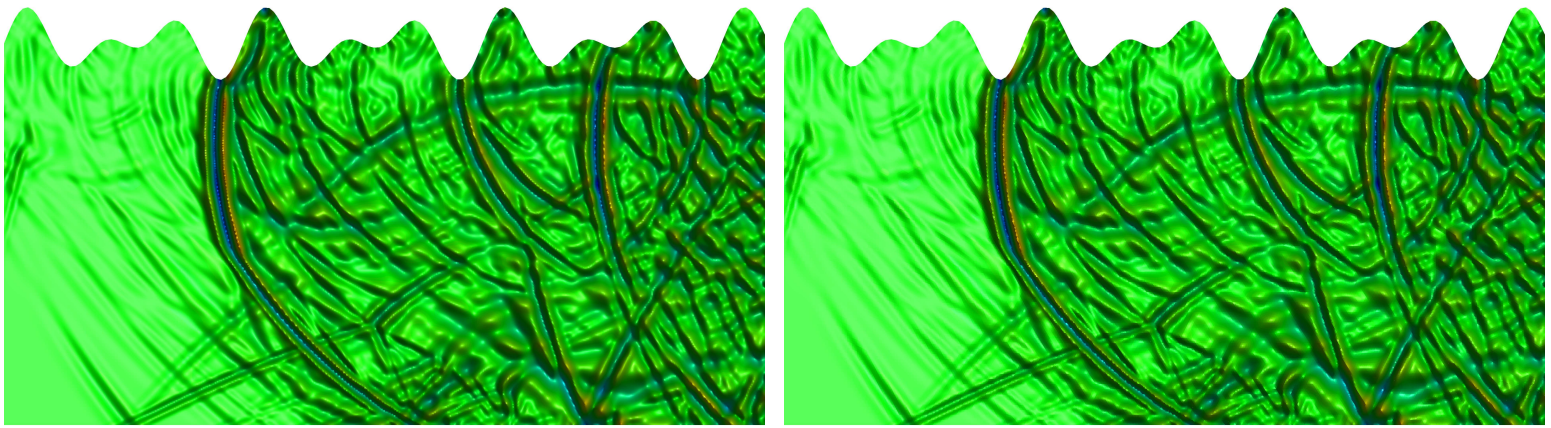

Numerical experiments

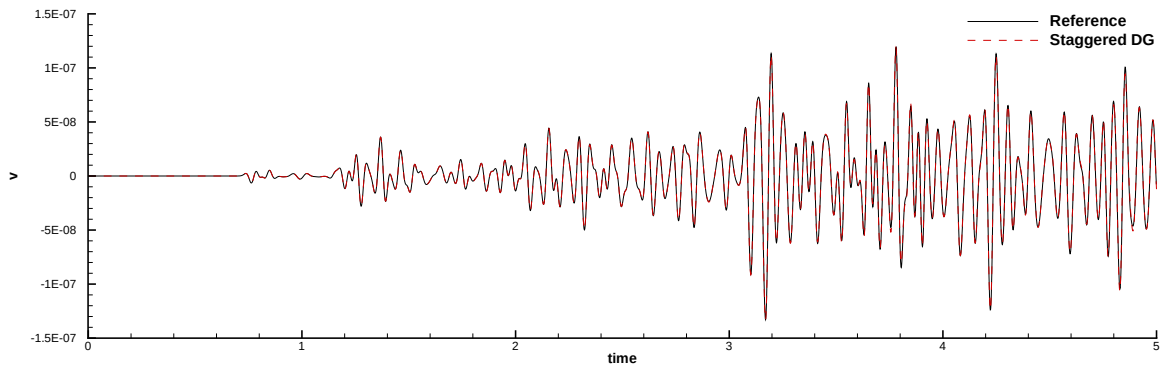

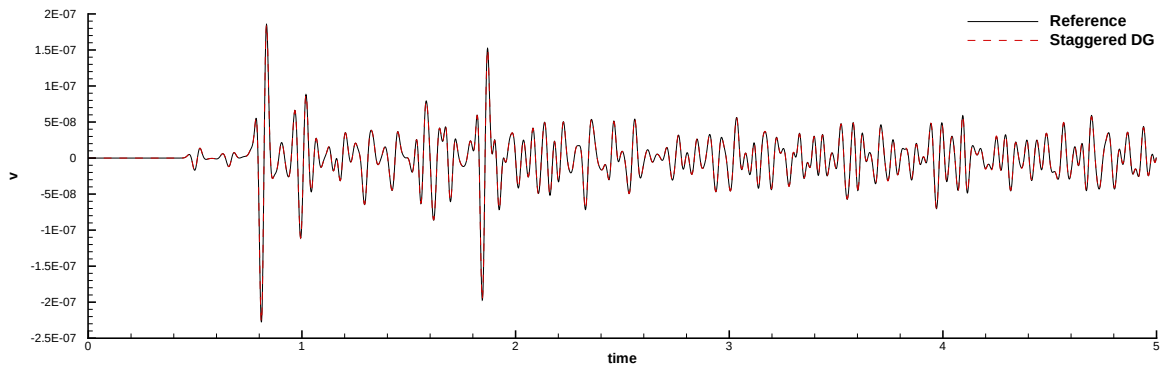

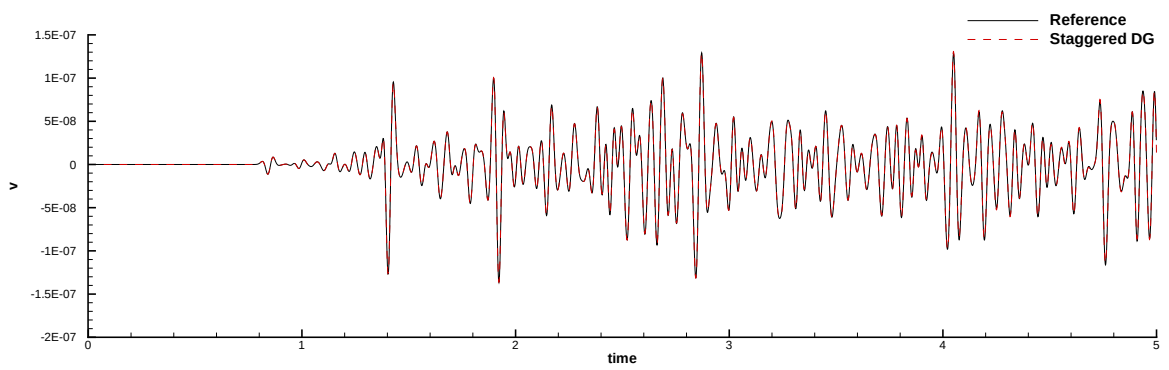

Numerical experiments

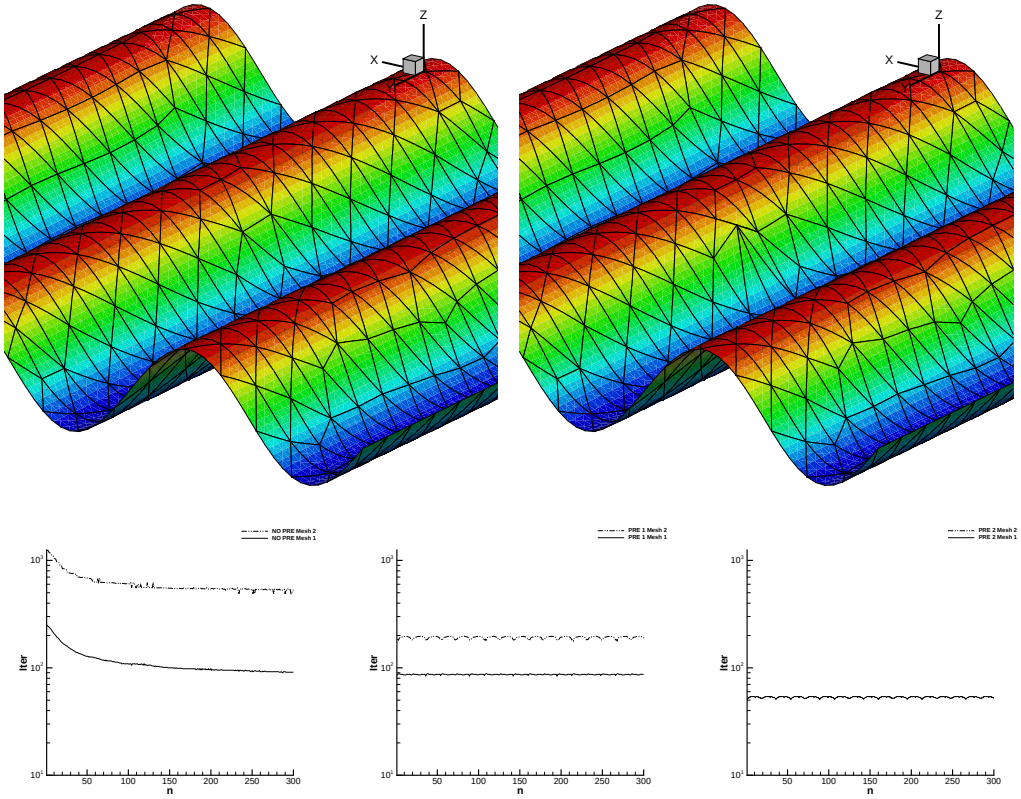

Number of average iterations needed for the GMRES algorithm with different preconditioners on the uniform unstructured grid (mesh 1) and the one containing the sliver elements (mesh 2) with $(p, p_\gamma) = (4, 2)$.

	Iter. Mesh 1	Iter. Mesh 2	Factor
None	112.59	611.95	5.43
Pre 1	86.73	191.77	2.21
Pre 2	53.27	53.38	1.00

Numerical experiments

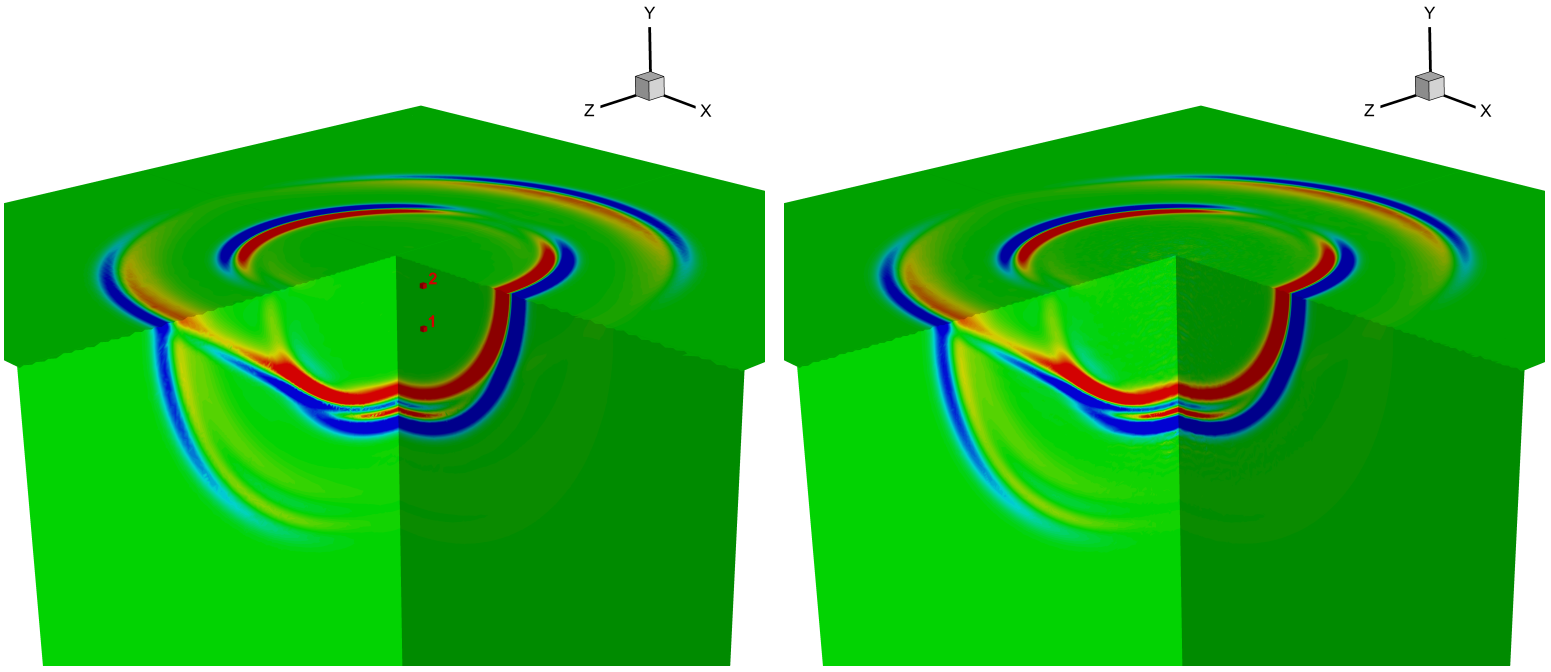

Numerical experiments

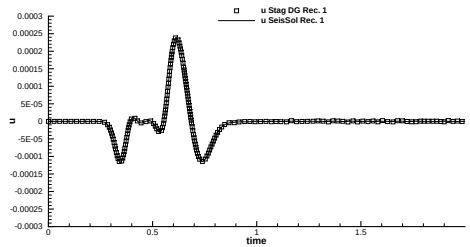

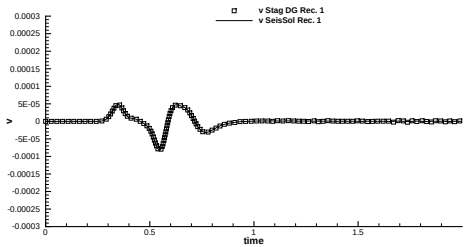

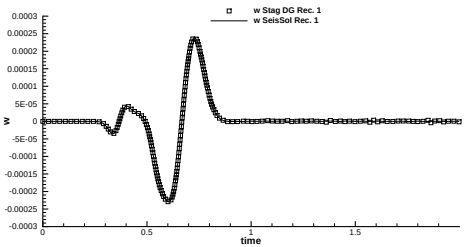

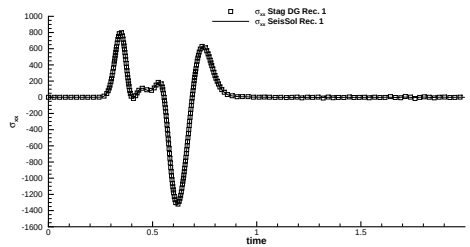

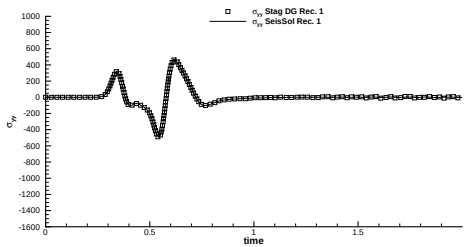

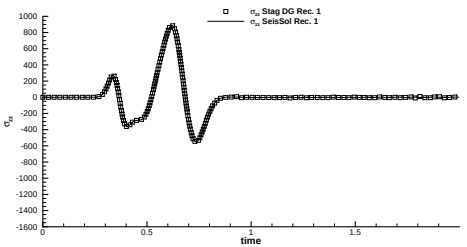

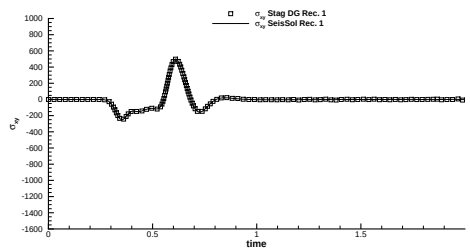

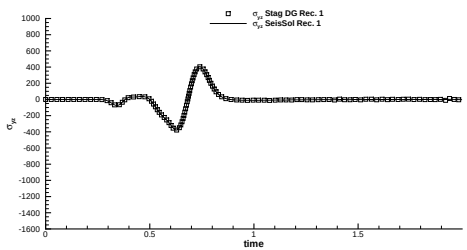

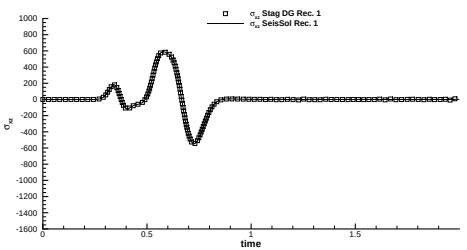

Numerical experiments

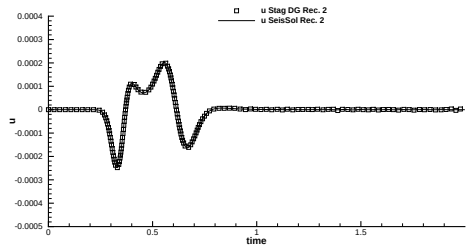

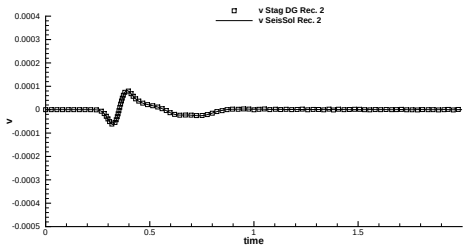

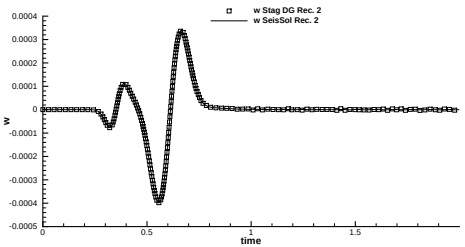

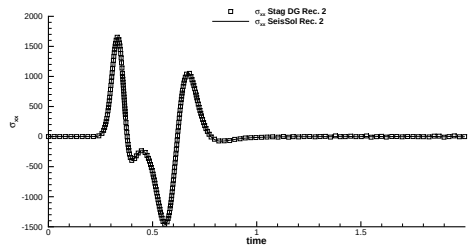

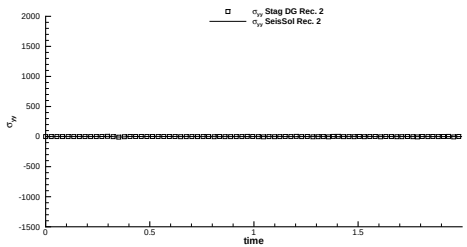

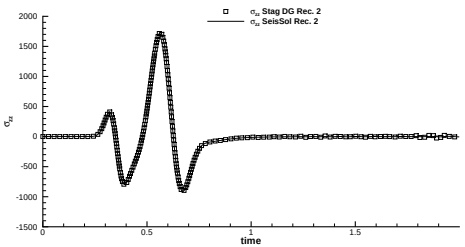

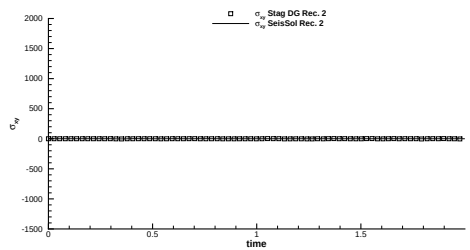

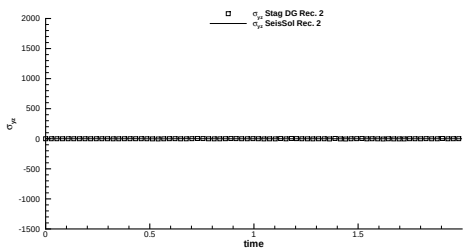

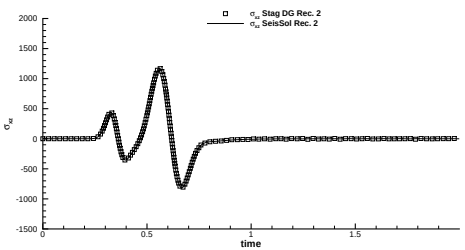

Numerical experiments

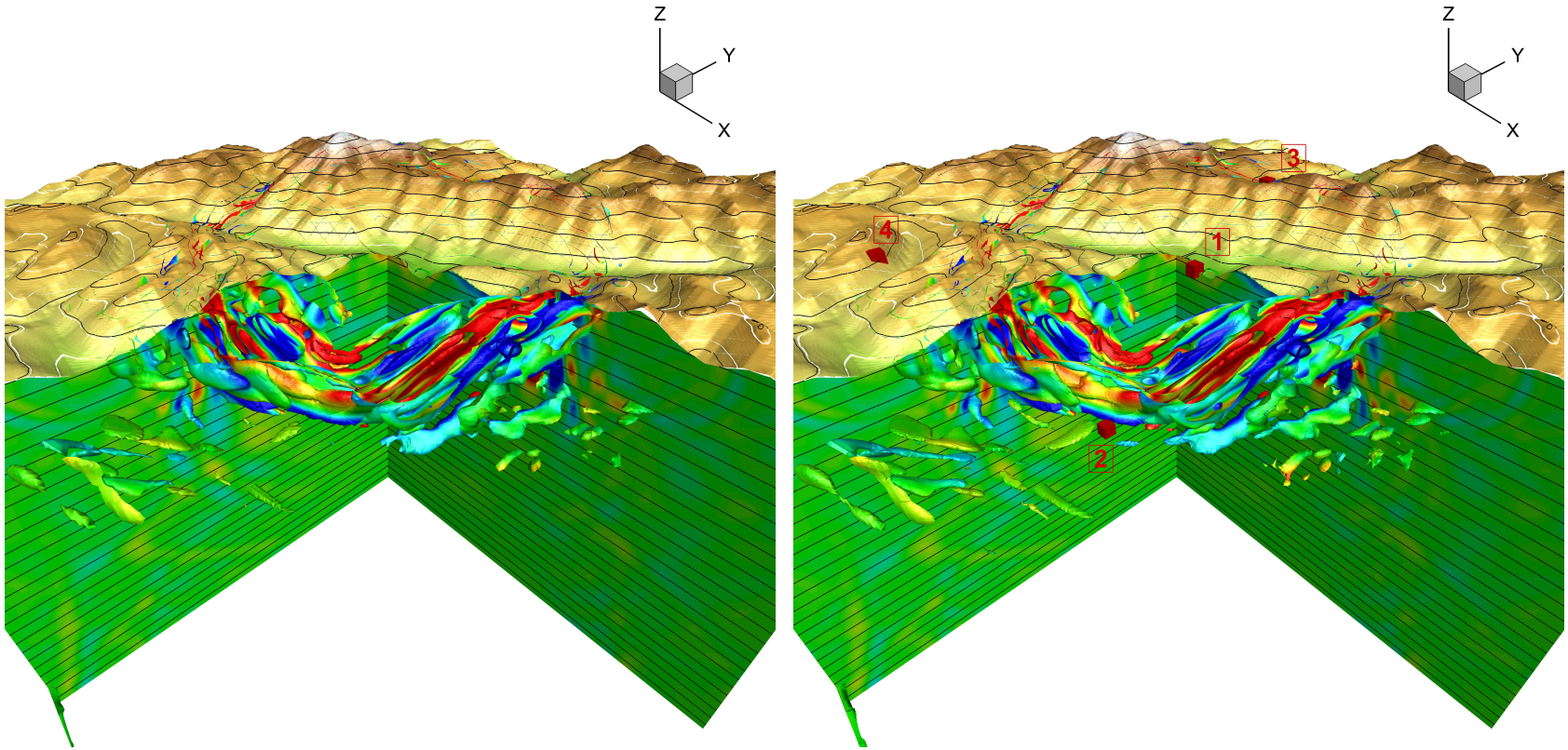

Numerical experiments

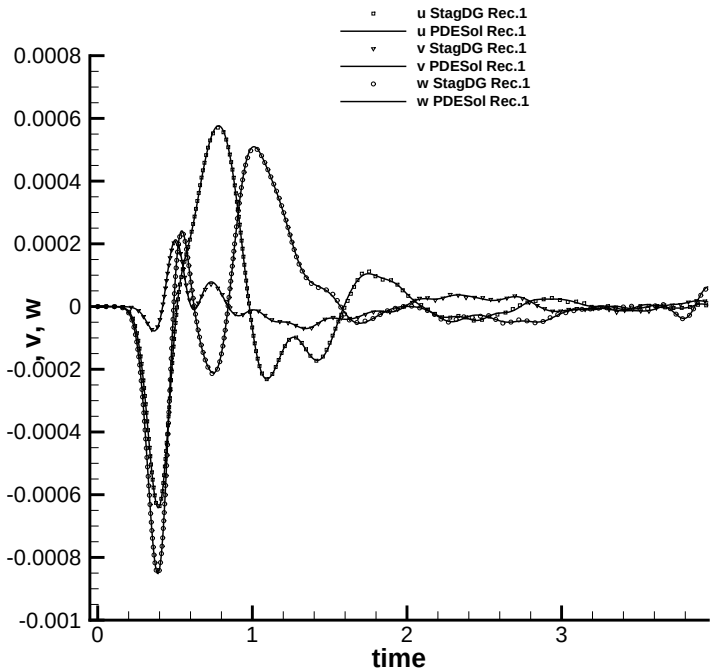

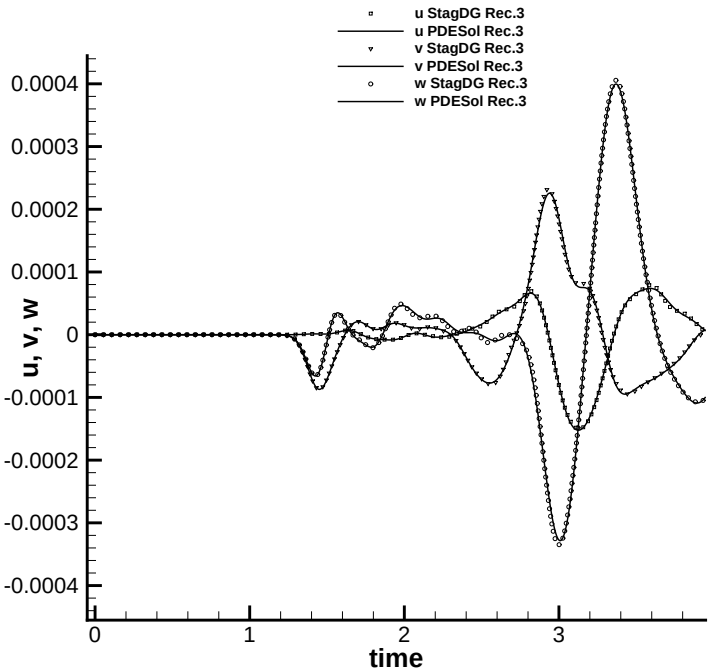

Main results

Main results

- Arbitrary high order method for the two and three-dimensional linear elasticity;
- The grid can be eventually curved;
- High order is achieved with a very small stencil;
- for $p_\gamma = 0$ the main system results symmetric and positive-definite;
- The method is energy stable $\forall p, p_\gamma$,
- For the special case of a Crank-Nicolson time discretization, the method is proven to be exactly energy conserving.

References

M. Tavelli and M. Dumbser, *Arbitrary high order accurate space–time discontinuous Galerkin finite element schemes on staggered unstructured meshes for linear elasticity*, Journal of computational physics, 2018

M. Tavelli and M. Dumbser, *A pressure-based semi-implicit space-time discontinuous Galerkin method on staggered unstructured meshes for the solution of the compressible Navier-Stokes equations at all Mach numbers*, Journal of computational physics, 2017

Diffuse Interface approach

Diffuse interface approach

We address the problem of geometrically complex free surface boundary conditions for seismic wave propagation problems with a novel diffuse interface method (DIM) on adaptive Cartesian meshes (AMR) that consists in the introduction of a characteristic function $0 \leq \alpha \leq 1$ which identifies the location of the solid medium and the surrounding air (or vacuum) and thus implicitly defines the location of the free surface boundary.

Diffuse interface approach

We address the problem of geometrically complex free surface boundary conditions for seismic wave propagation problems with a novel diffuse interface method (DIM) on adaptive Cartesian meshes (AMR) that consists in the introduction of a characteristic function $0 \leq \alpha \leq 1$ which identifies the location of the solid medium and the surrounding air (or vacuum) and thus implicitly defines the location of the free surface boundary.

$$\frac{\partial \boldsymbol{\sigma}}{\partial t} - \mathbf{E}(\lambda,\mu)\cdot\frac{1}{\alpha}\nabla(\alpha \boldsymbol{v}) + \frac{1}{\alpha}\mathbf{E}(\lambda,\mu)\cdot \boldsymbol{v}\otimes\nabla\alpha = 0,$$

$$\frac{\partial \alpha \boldsymbol{v}}{\partial t} - \frac{\alpha}{\rho}\nabla\cdot\boldsymbol{\sigma} - \frac{1}{\rho}\sigma\nabla\alpha = 0,$$

$$\frac{\partial \alpha}{\partial t} = 0. \frac{\partial \lambda}{\partial t} = 0, \qquad \frac{\partial \mu}{\partial t} = 0, \qquad \frac{\partial \rho}{\partial t} = 0.$$

Diffuse interface approach

$$\frac{\partial \mathbf{Q}}{\partial t} + \mathbf{B}_1(\mathcal{Q})\frac{\partial \mathbf{Q}}{\partial x} + \mathbf{B}_2(\mathcal{Q})\frac{\partial \mathbf{Q}}{\partial y} + \mathbf{B}_3(\mathcal{Q})\frac{\partial \mathbf{Q}}{\partial z} = 0,$$

$$\mathbf{Q} = \left(\sigma_{xx}, \sigma_{yy}, \sigma_{zz}, \sigma_{xy}, \sigma_{yz}, \sigma_{xz}, \alpha u, \alpha v, \alpha w, \lambda, \mu, \rho, \alpha\right)^\top,$$

Diffuse interface approach

$$\mathbf{B}_1 = \begin{pmatrix}
0 & 0 & 0 & 0 & 0 & 0 & -\frac{1}{\alpha}(\lambda+2\mu) & 0 & 0 & 0 & 0 & 0 & \frac{1}{\alpha}(\lambda+2\mu)u \\
0 & 0 & 0 & 0 & 0 & 0 & -\frac{1}{\alpha}\lambda & 0 & 0 & 0 & 0 & 0 & \frac{1}{\alpha}\lambda u \\
0 & 0 & 0 & 0 & 0 & 0 & -\frac{1}{\alpha}\lambda & 0 & 0 & 0 & 0 & 0 & \frac{1}{\alpha}\lambda u \\
0 & 0 & 0 & 0 & 0 & 0 & 0 & -\frac{1}{\alpha}\mu & 0 & 0 & 0 & 0 & \frac{1}{\alpha}\mu v \\
0 & 0 & 0 & 0 & 0 & 0 & 0 & 0 & 0 & 0 & 0 & 0 & 0 \\
0 & 0 & 0 & 0 & 0 & 0 & 0 & 0 & -\frac{1}{\alpha}\mu & 0 & 0 & 0 & \frac{1}{\alpha}\mu w \\
-\frac{\alpha}{\rho} & 0 & 0 & 0 & 0 & 0 & 0 & 0 & 0 & 0 & 0 & 0 & -\frac{1}{\rho}\sigma_{xx} \\
0 & 0 & 0 & -\frac{\alpha}{\rho} & 0 & 0 & 0 & 0 & 0 & 0 & 0 & 0 & -\frac{1}{\rho}\sigma_{xy} \\
0 & 0 & 0 & 0 & 0 & -\frac{\alpha}{\rho} & 0 & 0 & 0 & 0 & 0 & 0 & -\frac{1}{\rho}\sigma_{xz} \\
0 & 0 & 0 & 0 & 0 & 0 & 0 & 0 & 0 & 0 & 0 & 0 & 0 \\
0 & 0 & 0 & 0 & 0 & 0 & 0 & 0 & 0 & 0 & 0 & 0 & 0 \\
0 & 0 & 0 & 0 & 0 & 0 & 0 & 0 & 0 & 0 & 0 & 0 & 0 \\
0 & 0 & 0 & 0 & 0 & 0 & 0 & 0 & 0 & 0 & 0 & 0 & 0
\end{pmatrix},$$

Diffuse interface approach

The matrix of right eigenvectors of the matrix $\mathbf{B}_1$ is given by

$$\mathbf{R} = \begin{pmatrix}
\rho c_p^2 & 0 & 0 & 0 & 0 & 0 & 0 & 0 & 0 & -\sigma_{xx} & 0 & 0 & \rho c_p^2 \\
\rho(c_p^2 - 2c_s^2) & 0 & 0 & 1 & 0 & 0 & 0 & 0 & 0 & 0 & 0 & 0 & \rho(c_p^2 - 2c_s^2) \\
\rho(c_p^2 - 2c_s^2) & 0 & 0 & 0 & 1 & 0 & 0 & 0 & 0 & 0 & 0 & 0 & \rho(c_p^2 - 2c_s^2) \\
0 & \rho c_s^2 & 0 & 0 & 0 & 0 & 0 & 0 & 0 & -\sigma_{xy} & 0 & \rho c_s^2 & 0 \\
0 & 0 & 0 & 0 & 0 & 1 & 0 & 0 & 0 & 0 & 0 & 0 & 0 \\
0 & 0 & \rho c_s^2 & 0 & 0 & 0 & 0 & 0 & 0 & -\sigma_{xz} & \rho c_s^2 & 0 & 0 \\
c_p & 0 & 0 & 0 & 0 & 0 & 0 & 0 & 0 & \alpha u & 0 & 0 & -c_p \\
0 & c_s & 0 & 0 & 0 & 0 & 0 & 0 & 0 & \alpha v & 0 & -c_s & 0 \\
0 & 0 & c_s & 0 & 0 & 0 & 0 & 0 & 0 & \alpha w & -c_s & 0 & 0 \\
0 & 0 & 0 & 0 & 0 & 0 & 0 & 0 & 1 & 0 & 0 & 0 & 0 \\
0 & 0 & 0 & 0 & 0 & 0 & 0 & 1 & 0 & 0 & 0 & 0 & 0 \\
0 & 0 & 0 & 0 & 0 & 0 & 1 & 0 & 0 & 0 & 0 & 0 & 0 \\
0 & 0 & 0 & 0 & 0 & 0 & 0 & 0 & 0 & \alpha & 0 & 0 & 0
\end{pmatrix}.$$

The eigenvalues associated with the matrix $\mathbf{B}_1$ are

$$\lambda_1 = -c_p, \quad \lambda_{2,3} = -c_s, \quad \lambda_{4,5,6,7,8,9,10} = 0, \quad \lambda_{11,12} = +c_s, \quad \lambda_{13} = +c_p,$$

where

$$c_p = \sqrt{\frac{\lambda + 2\mu}{\rho}} \qquad \text{and} \qquad c_s = \sqrt{\frac{\mu}{\rho}}$$

are the $p-$ and $s-$ wave velocities, respectively.

Diffuse interface approach

$$
\begin{aligned}
\mathbf{Q}_L &= (\sigma_{xx}^L, \sigma_{yy}^L, \sigma_{zz}^L, \sigma_{xy}^L, \sigma_{yz}^L, \sigma_{xz}^L, u^L, v^L, w^L, \lambda, \mu, \rho, 1), \\
\mathbf{Q}_R &= (\sigma_{xx}^R, \sigma_{yy}^R, \sigma_{zz}^R, \sigma_{xy}^R, \sigma_{yz}^R, \sigma_{xz}^R, 0, 0, 0, \lambda, \mu, \rho, 0).
\end{aligned}
$$

$$\Downarrow$$

$$
\begin{aligned}
\mathbf{Q}_{\text{God}} = \Bigg(& 0, \frac{\sigma_{xx}^L c_p^2 + 2\sigma_{xx}^L c_s^2 + \sigma_{yy} c_p^2}{c_p^2}, \frac{\sigma_{xx}^L c_p^2 + 2\sigma_{xx}^L c_s^2 + \sigma_{zz} c_p^2}{c_p^2}, 0, \sigma_{yz}^L, 0, \\
& \frac{c_p \rho u^L - \sigma_{xx}^L}{c_p \rho}, \frac{c_s \rho v^L - \sigma_{xy}^L}{c_s \rho}, \frac{c_s \rho w^L - \sigma_{xz}^L}{c_s \rho}, \lambda, \mu, \rho, 1 \Bigg),
\end{aligned}
$$

Diffuse interface approach

$$\frac{\partial \mathbf{Q}}{\partial t} + \mathbf{B}_1(\mathcal{Q})\frac{\partial \mathbf{Q}}{\partial x} + \mathbf{B}_2(\mathcal{Q})\frac{\partial \mathbf{Q}}{\partial y} + \mathbf{B}_3(\mathcal{Q})\frac{\partial \mathbf{Q}}{\partial z} = 0,$$

Numerical scheme

- Arbitrary high order accurate (in space and time) explicit ADER-DG schemes on Cartesian meshes;
- Adaptive mesh refinement (AMR);
- *a posteriori* subcell finite volume limiter with a very robust second order TVD scheme.

$$\Delta t < \frac{\mathrm{CFL}}{d}\frac{h}{2N+1}\frac{1}{|\lambda_{max}|},$$

Numerical experiments

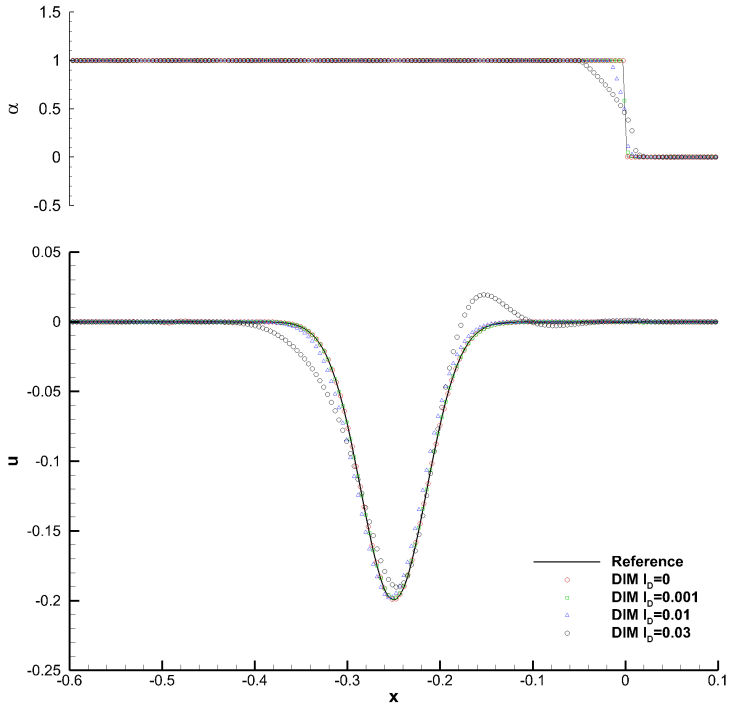

Finite interface thickness $l_D \geq 0$;
shifting parameter η;

$$\xi(r) = \begin{cases} 1 & \text{if} \quad r > (1+\eta) l_D, \\ 0 & \text{if} \quad r < -(1-\eta) l_D, \\ \frac{r+(1-\eta) l_D}{2 l_D} & \text{if} \quad r \in [-(1-\eta) l_D, (1+\eta) l_D]. \end{cases}$$

$$\alpha(r) = (1 - \xi(r))^{p_d},$$

$$\alpha^{-1} \cong \frac{\alpha}{\alpha^2 + \epsilon(\alpha)} \qquad \epsilon(\alpha) = \epsilon_0 (1 - \alpha)$$

Numerical experiments

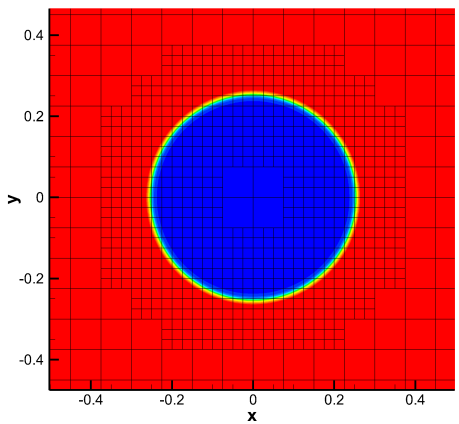

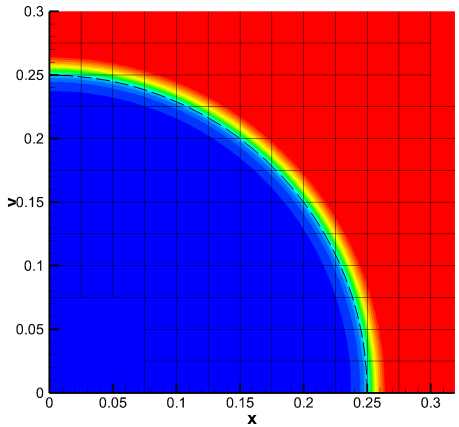

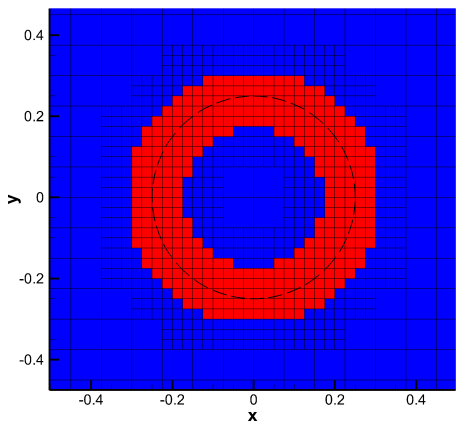

Numerical experiments

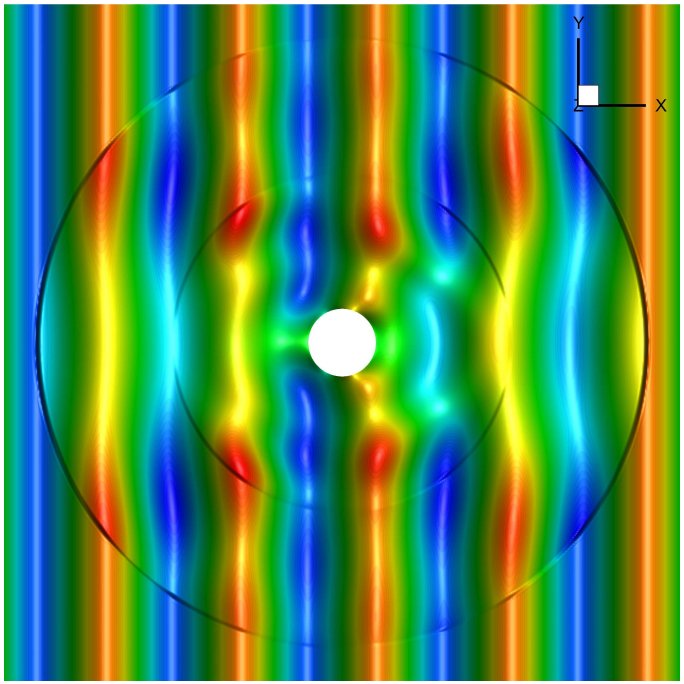

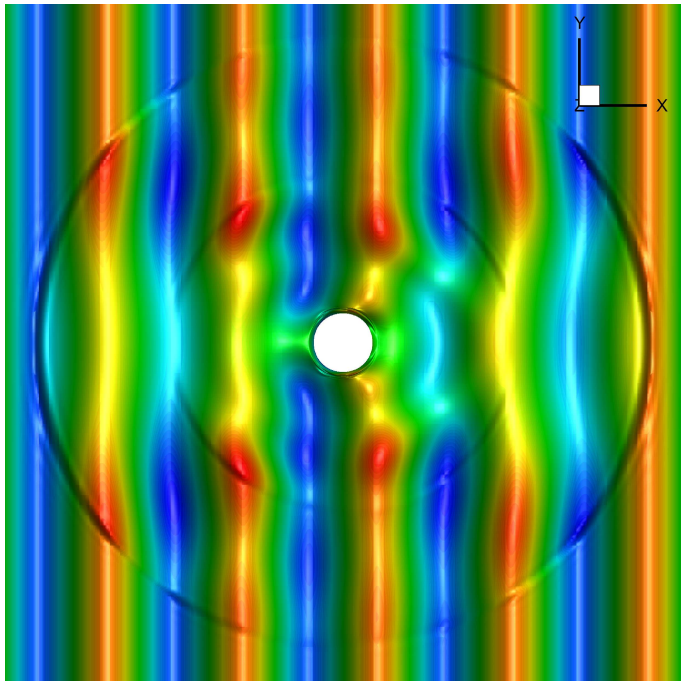

Numerical experiments

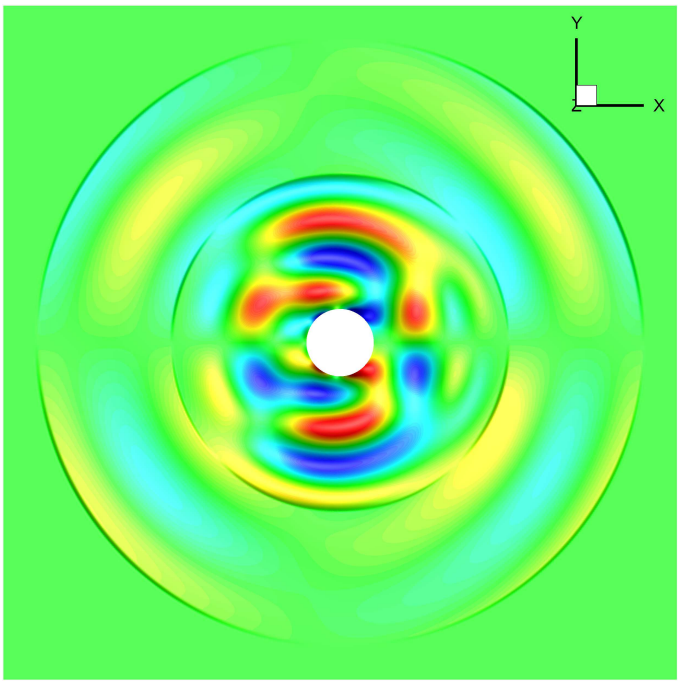

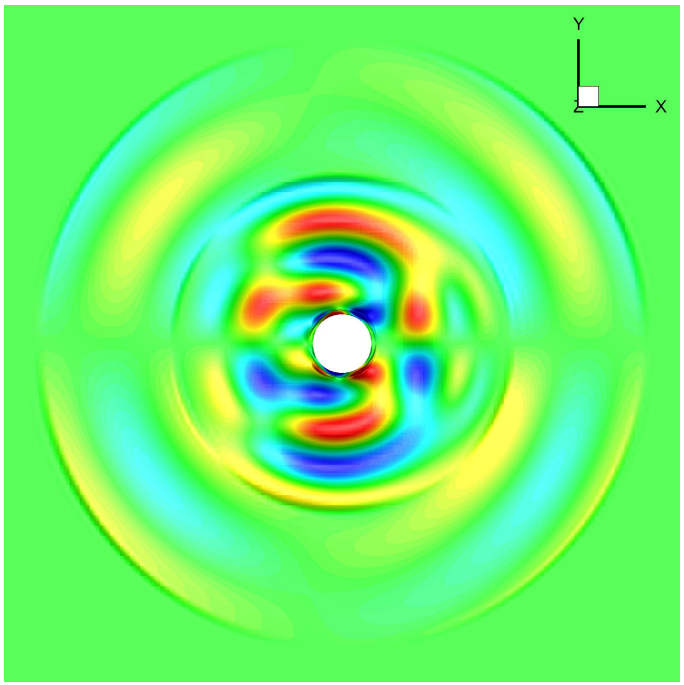

Numerical experiments

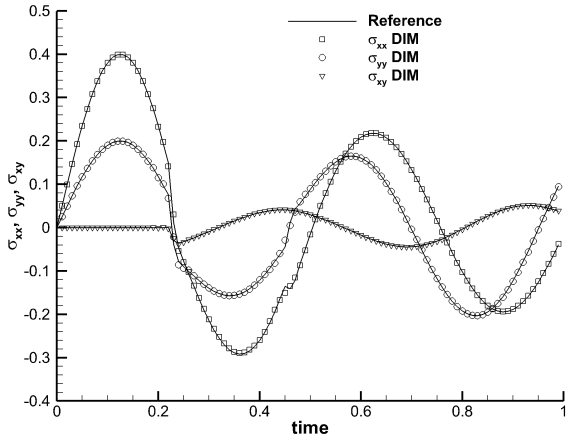

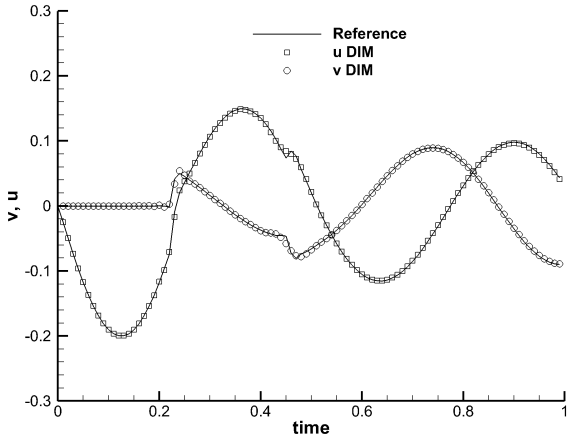

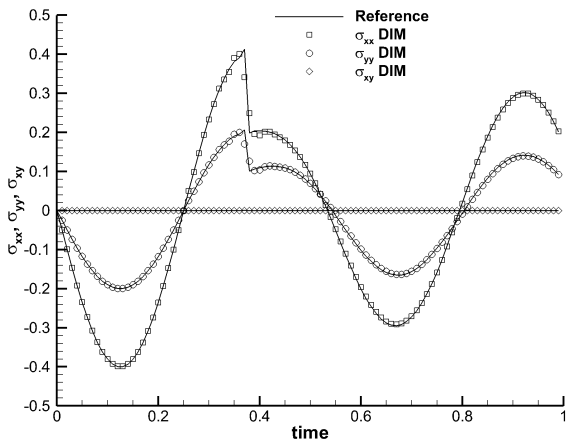

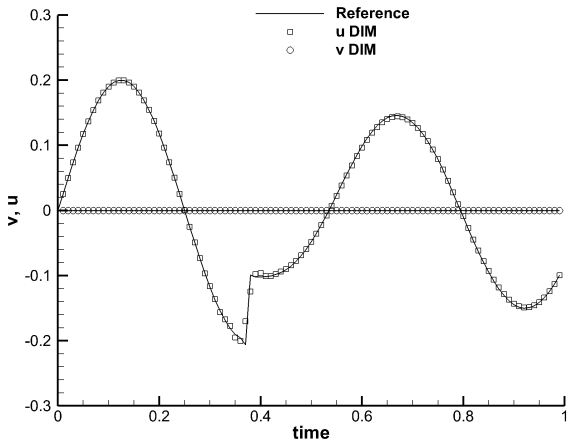

Numerical experiments

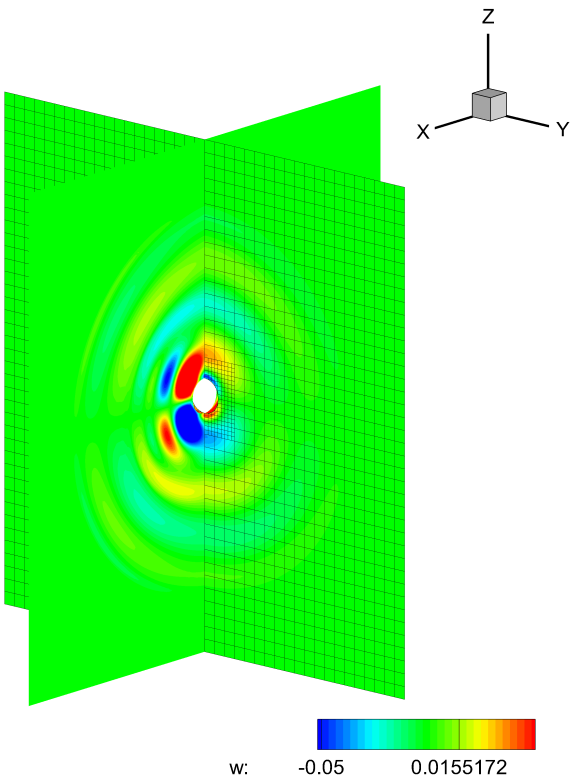

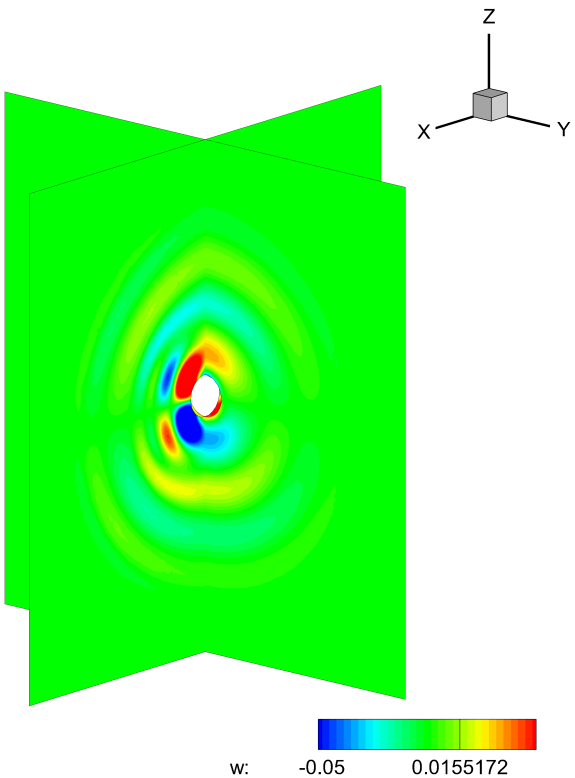

Numerical experiments

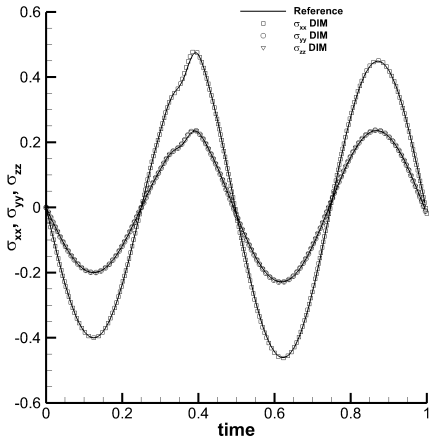

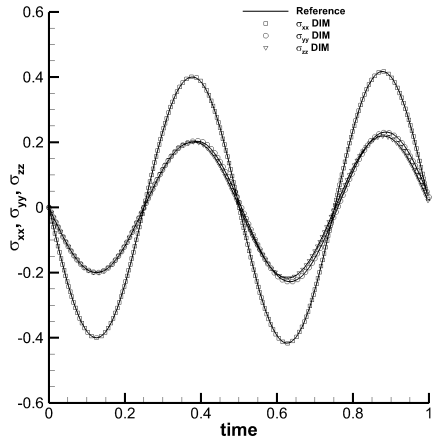

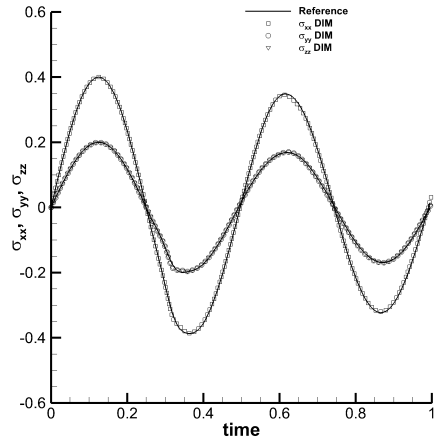

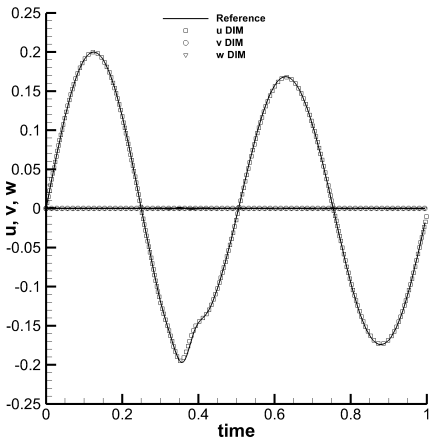

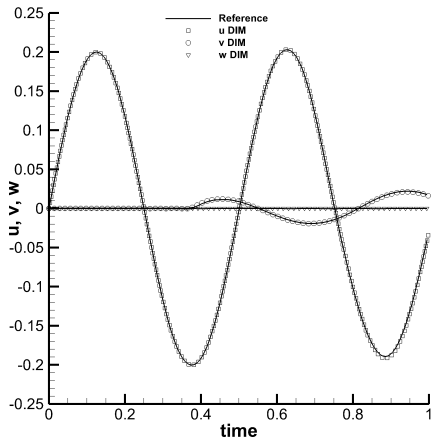

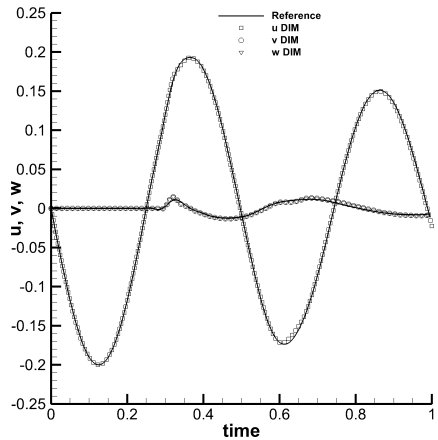

Numerical experiments

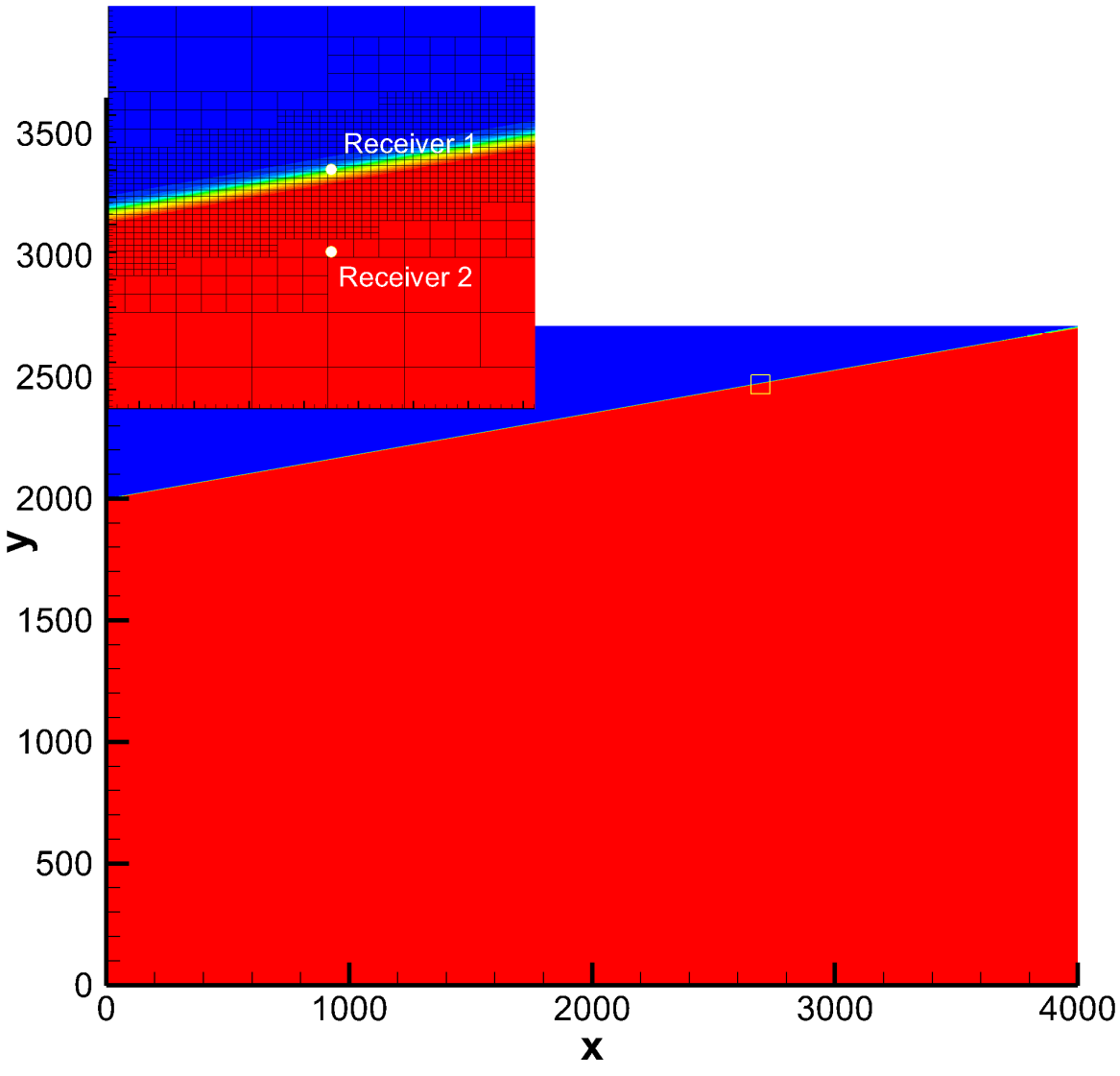

Numerical experiments

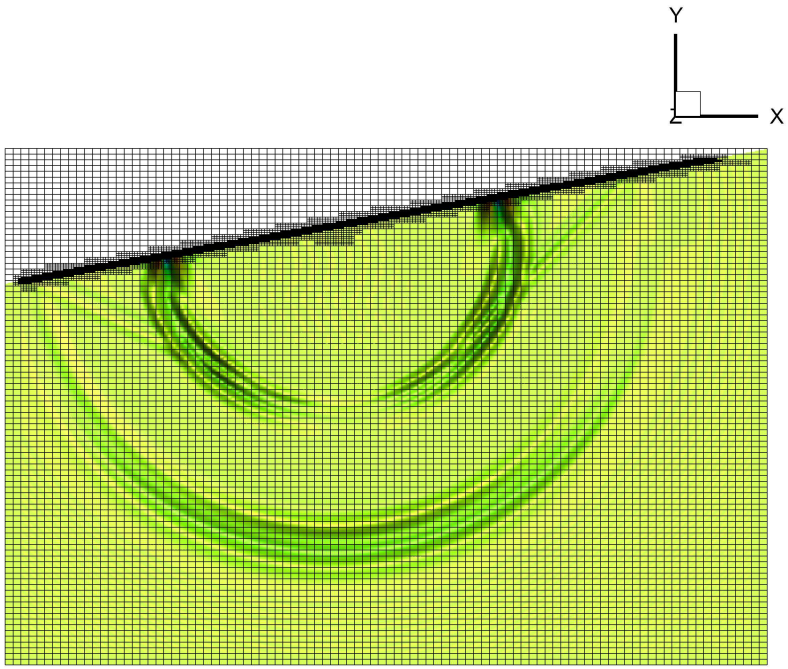

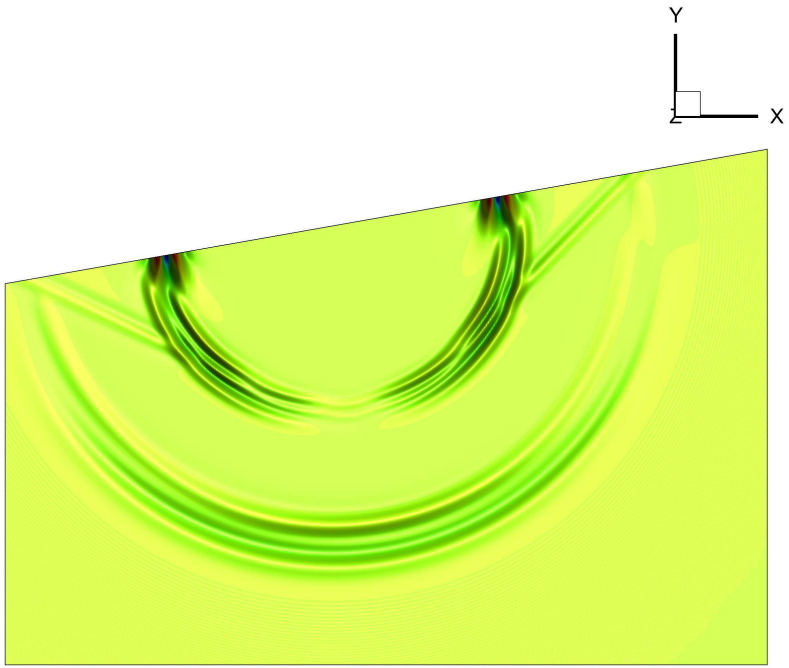

Numerical experiments

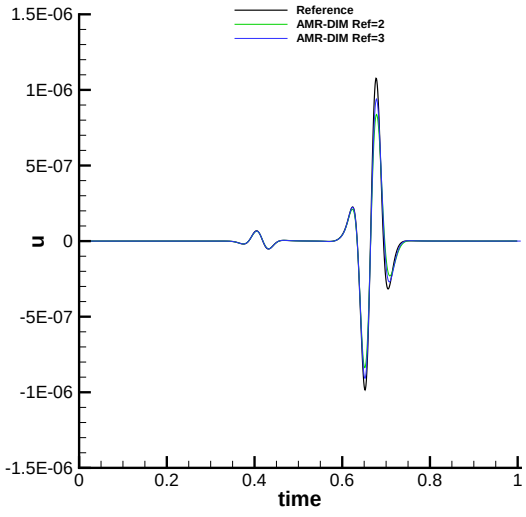

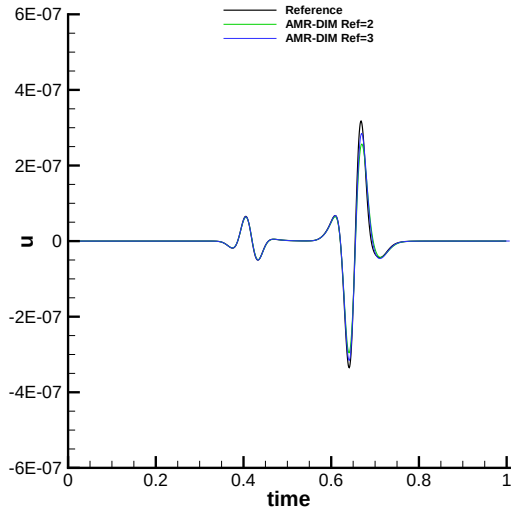

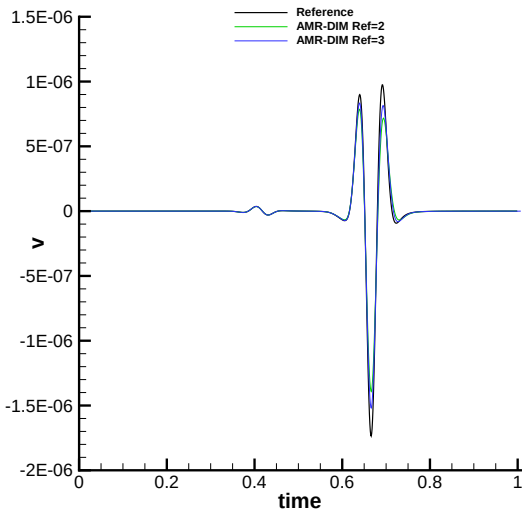

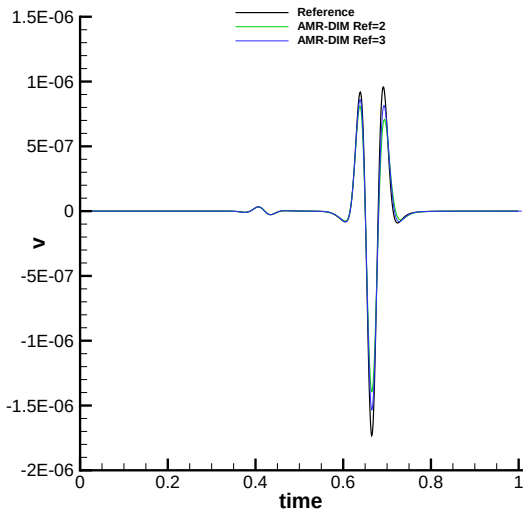

Numerical experiments

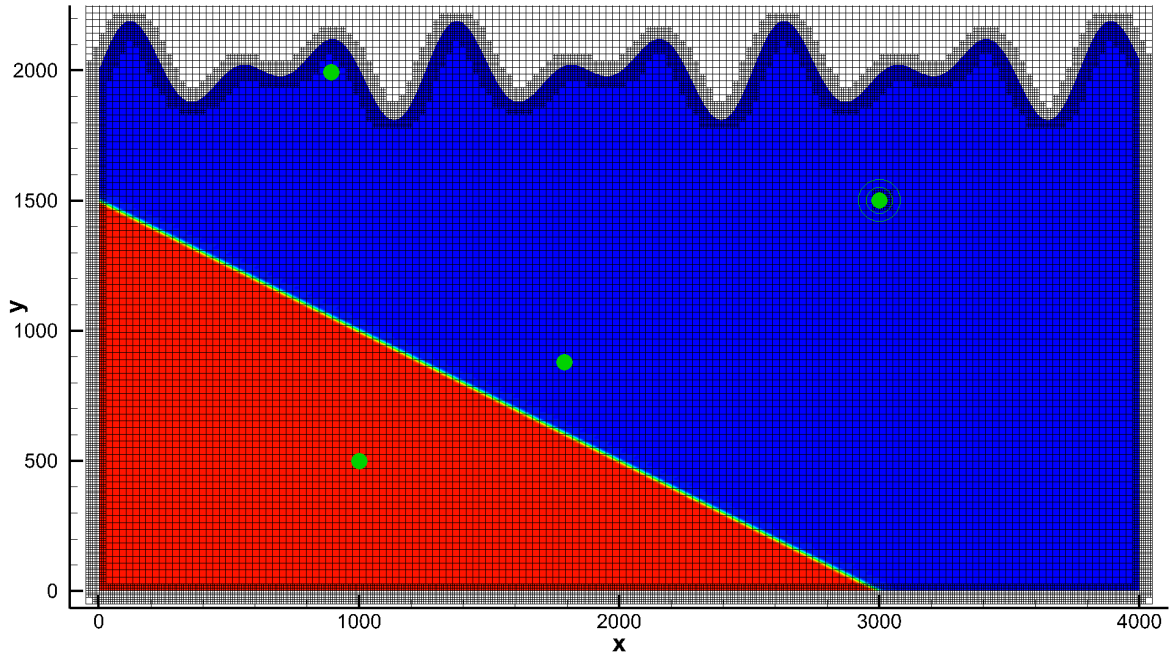

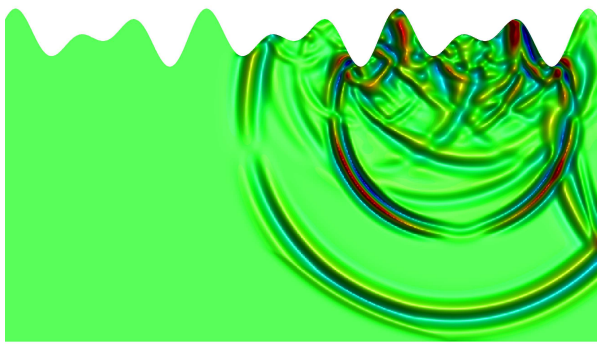

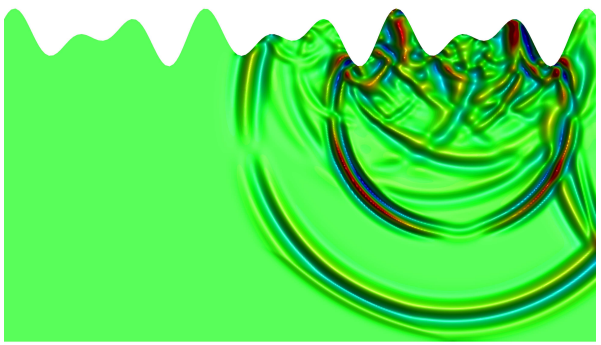

Numerical experiments

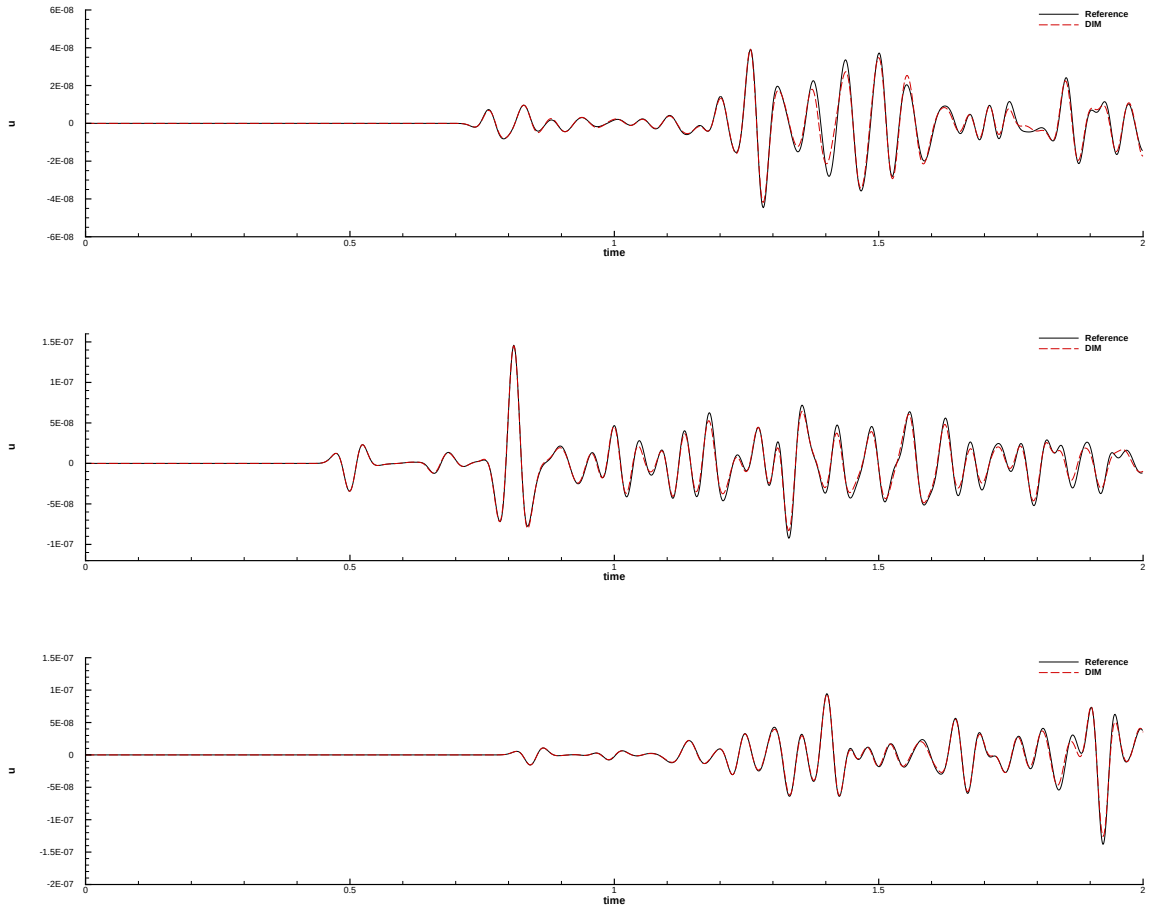

Numerical experiments

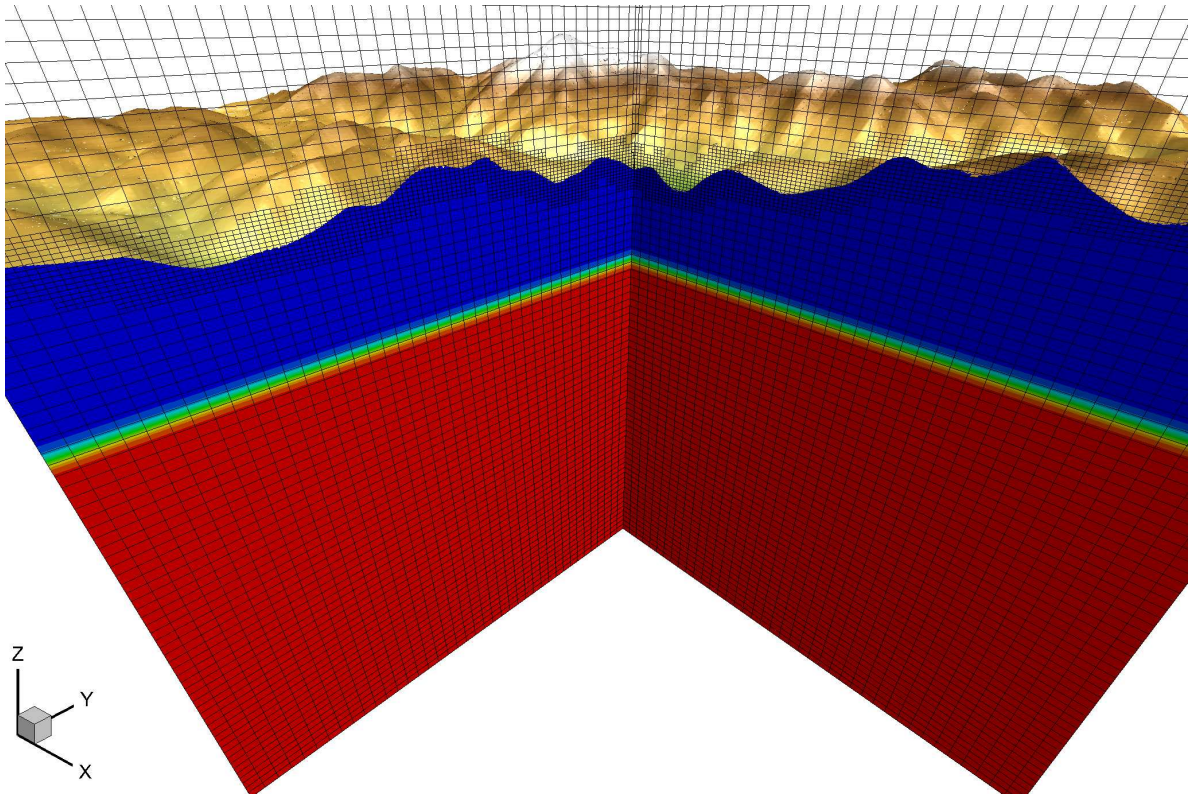

Numerical experiments

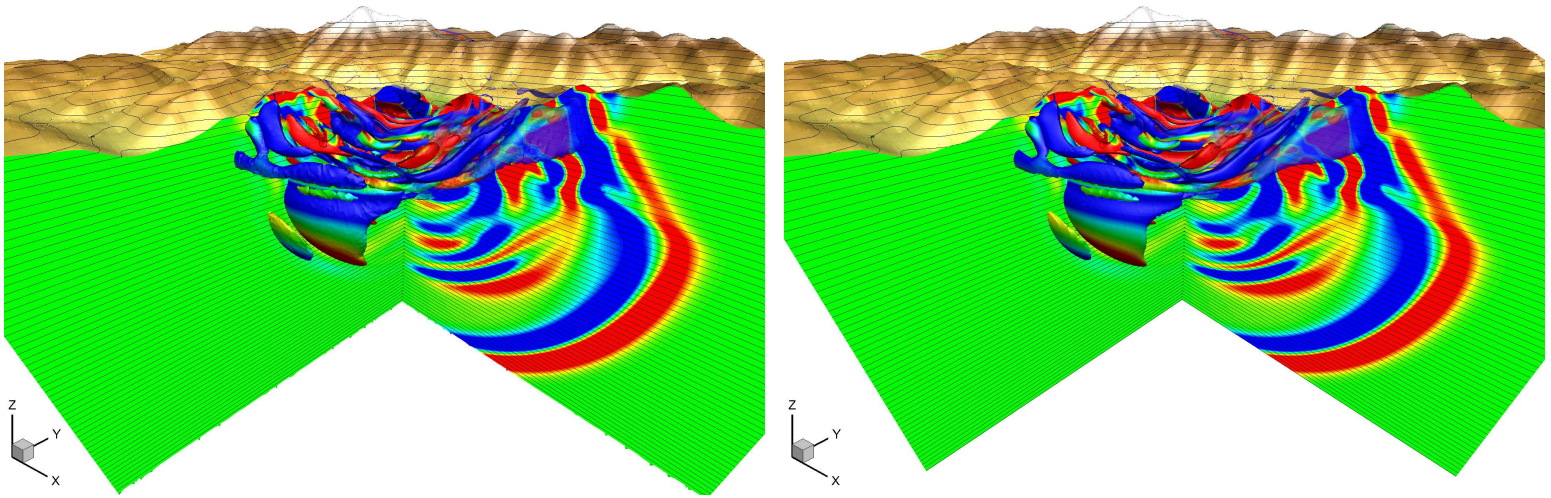

Numerical experiments

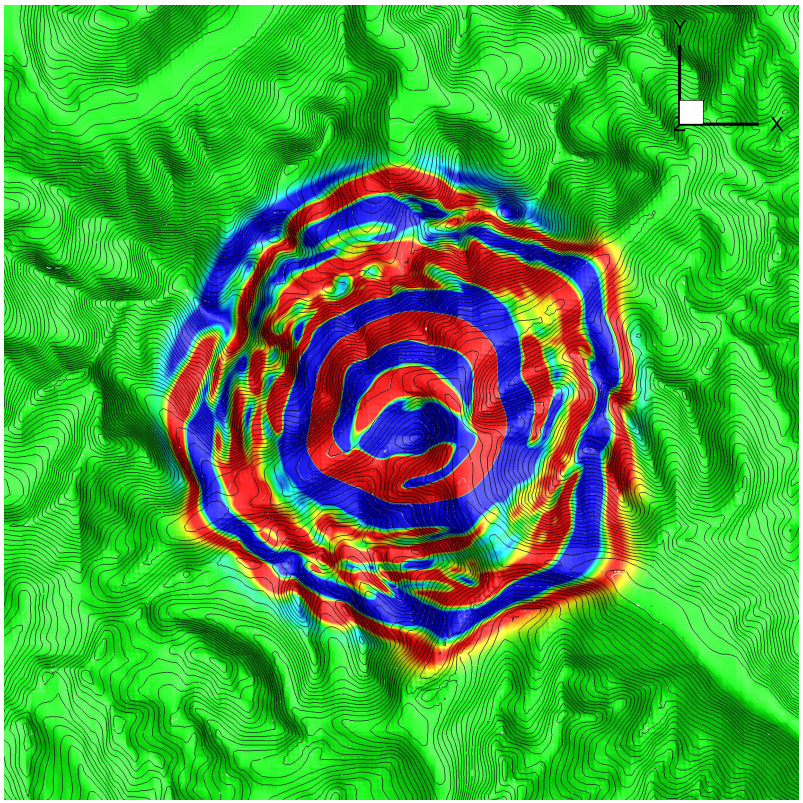

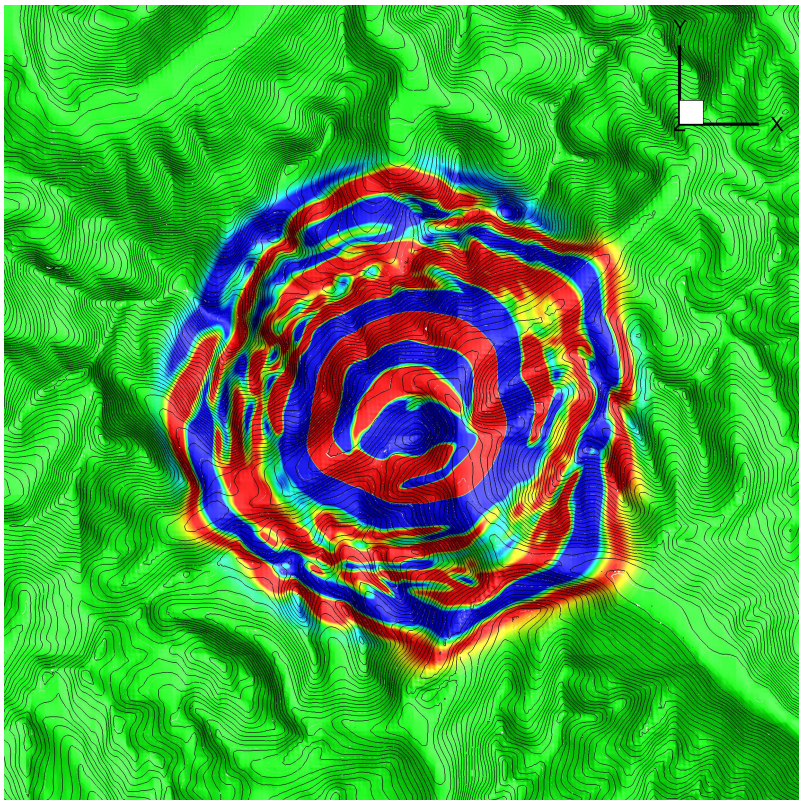

Numerical experiments

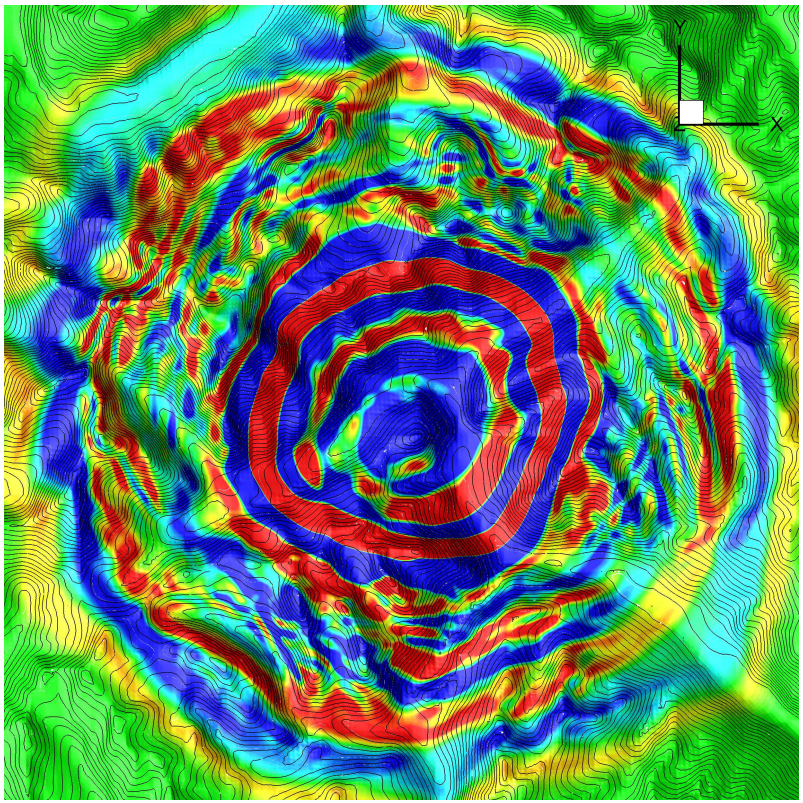

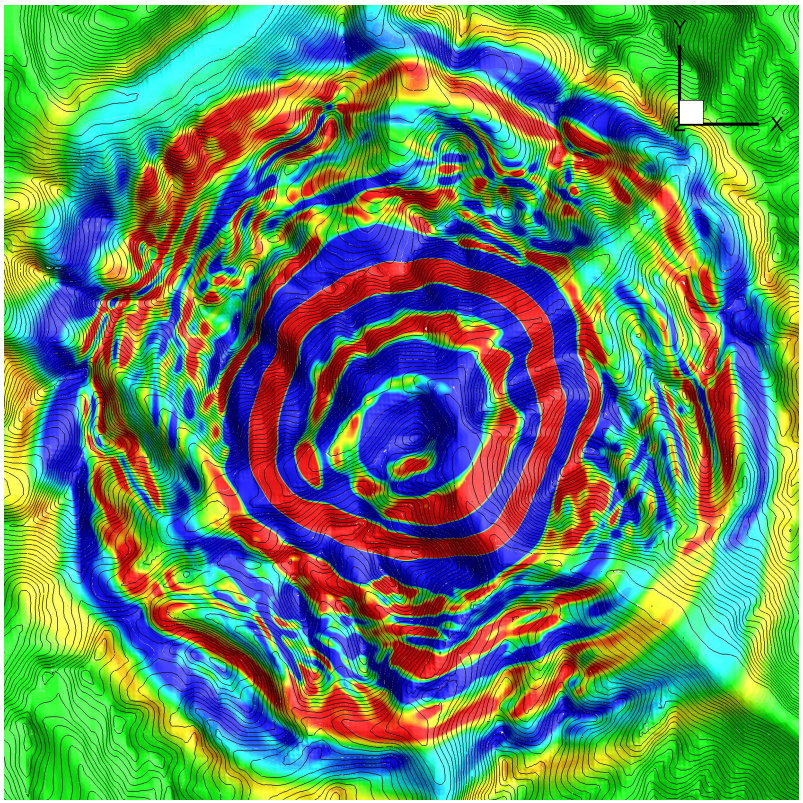

Numerical experiments

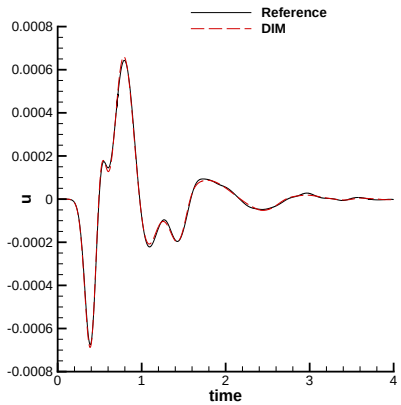

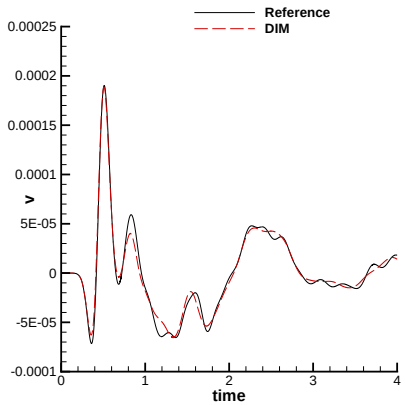

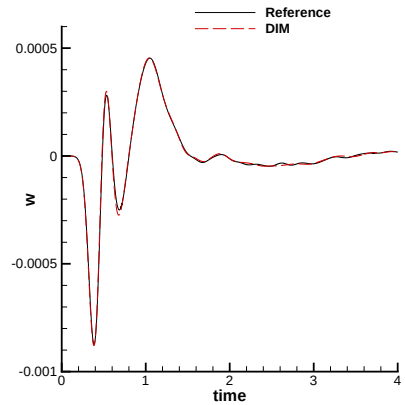

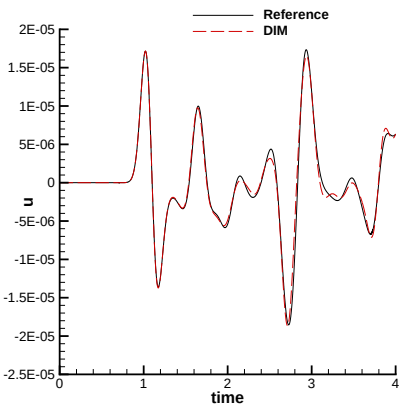

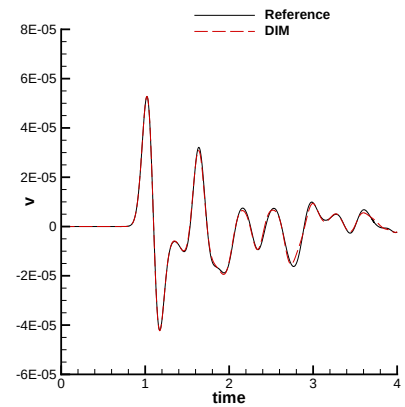

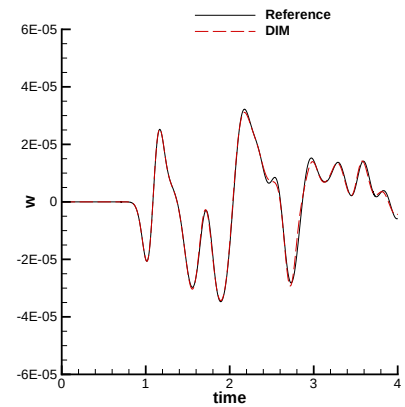

Main results

Main results

- A novel diffuse interface method (DIM) for the simulation of seismic wave propagation for arbitrary complex geometries;
- The free surface topology does not affect the CFL time restriction (no sliver elements) since α has no influence on the eigenvalues of the governing PDE system.
- It does not require any external mesh generation tools or any manual interaction with the user.

References

M. Tavelli, M. Dumbser, D. E. Charrier, L. Rannabauer, T. Weinzierl, M. Bader, *A simple diffuse interface approach on adaptive Cartesian grids for the linear elastic wave equations with complex topography* , Journal of computational physics, submitted to, 2018

Acknowledgements

Thank you for the attention

This research was funded by the European Union's Horizon 2020 Research and Innovation Programme under the project *ExaHyPE*, grant no. 671698 (call FETHPC-1-2014). The 3D simulations were performed on the HazelHen supercomputer at the HLRS in Stuttgart, Germany and on the SuperMUC supercomputer at the LRZ in Garching, Germany.

Appendix

$$
\begin{aligned}
\frac{\partial}{\partial t}\left(\alpha_s \rho_s\right) + \nabla \cdot \left(\alpha_s \rho_s \mathbf{v}_s\right) &= 0, \\
\frac{\partial}{\partial t}\left(\alpha_s \rho_s \mathbf{v}_s\right) + \nabla \cdot \left(\alpha_s \rho_s \mathbf{v}_s \otimes \mathbf{v}_s + \alpha_s \boldsymbol{\sigma}_s\right) - \boldsymbol{\sigma}_I \nabla \alpha_s &= \alpha_s \rho_s \mathbf{S}_{v,s}, \\
\frac{\partial}{\partial t}\left(\alpha_s \rho_s E_s\right) + \nabla \cdot \left(\alpha_s \rho_s E_s \mathbf{v}_s + \alpha_s \boldsymbol{\sigma}_s \mathbf{v}_s\right) - \boldsymbol{\sigma}_I \nabla \alpha_s \cdot \mathbf{v}_I &= \alpha_s \rho_s \mathbf{S}_{v,s} \cdot \mathbf{v}_s, \\
\frac{\partial}{\partial t}\left(\alpha_g \rho_g\right) + \nabla \cdot \left(\alpha_g \rho_g \mathbf{v}_g\right) &= 0, \\
\frac{\partial}{\partial t}\left(\alpha_g \rho_g \mathbf{v}_g\right) + \nabla \cdot \left(\alpha_g \rho_g \mathbf{v}_g \otimes \mathbf{v}_g + \alpha_g \boldsymbol{\sigma}_g\right) - \boldsymbol{\sigma}_g \nabla \alpha_g &= \alpha_g \rho_g \mathbf{S}_{v,g}, \\
\frac{\partial}{\partial t}\left(\alpha_g \rho_g E_g\right) + \nabla \cdot \left(\alpha_g \rho_g E_g \mathbf{v}_g + \alpha_g \boldsymbol{\sigma}_g \mathbf{v}_g\right) - \boldsymbol{\sigma}_I \nabla \alpha_g \cdot \mathbf{v}_I &= \alpha_g \rho_g \mathbf{S}_{v,g} \cdot \mathbf{v}_g, \\
\frac{\partial}{\partial t}\alpha_s + \mathbf{v}_I \nabla \alpha_s &= 0. \qquad (1)
\end{aligned}
$$

Appendix

Assumptions:

- The interface between solid and gas is not moving, i.e. $\mathbf{v}_I = 0$;
- all evolution equations related to the gas phase can be neglected;
- we assume the density ρ_s of the solid phase to be constant in time;
- the nonlinear convective term $\alpha_s \rho_s \mathbf{v}_s \otimes \mathbf{v}_s$;
- boundary condition at the interface leads to $\boldsymbol{\sigma}_s \cdot \nabla \alpha_s = 0$.